Petroleum Science 21 (2024) 3446–3463

Contents lists available at ScienceDirect

Petroleum Science

journal homepage: www.keaipublishing.com/en/journals/petroleum-science

Original Paper

Curing kinetics and plugging mechanism of high strength curable resin plugging material

Jing-Bin Yang [a], Ying-Rui Bai [a, *], Jin-Sheng Sun [a, b], Kai-He Lv [a]

[a] School of Petroleum Engineering, China University of Petroleum (East China), Qingdao, 266580, Shandong, China
[b] CNPC Engineering Technology R&D Company Limited, Beijing, 102206, China

ARTICLE INFO

Article history:
Received 25 July 2023
Received in revised form
29 April 2024
Accepted 29 April 2024
Available online 3 May 2024

Edited by Jia-Jia Fei

Keywords:
Urea-formaldehyde resin
Rheological property
Curing property
Curing kinetics
Plugging mechanism

ABSTRACT

Lost circulation, a recurring peril during drilling operations, entails substantial loss of drilling fluid and dire consequences upon its infiltration into the formation. As drilling depth escalates, the formation temperature and pressure intensify, imposing exacting demands on plug materials. In this study, a kind of controllable curing resin with dense cross-network structure was prepared by the method of solution stepwise ring-opening polymerization. The resin plugging material investigated in this study is a continuous phase material that offers effortless injection, robust filling capabilities, exceptional retention, and underground curing or crosslinking with high strength. Its versatility is not constrained by fracture-cavity lose channels, making it suitable for fulfilling the essential needs of various fracture-cavity combinations when plugging fracture-cavity carbonate rocks. Notably, the curing duration can be fine-tuned within the span of 3–7 h, catering to the plugging of drilling fluid losing of diverse fracture dimensions. Experimental scrutiny encompassed the rheological properties and curing behavior of the resin plugging system, unraveling the intricacies of the curing process and establishing a cogent kinetic model. The experimental results show that the urea-formaldehyde resin plugging material has a tight chain or network structure. When the concentration of the urea-formaldehyde resin plugging system solution remains below 30%, the viscosity clocks in at a meager 10 mPa·s. Optimum curing transpires at 60 °C, showcasing impressive resilience to saline conditions. Remarkably, when immersed in a composite saltwater environment containing 50000 mg/L NaCl and 100000 mg/L $CaCl_2$, the urea-formaldehyde resin consolidates into an even more compact network structure, culminating in an outstanding compressive strength of 41.5 MPa. Through resolving the correlation between conversion and the apparent activation energy of the non-isothermal DSC curing reaction parameters, the study attests to the fulfillment of the kinetic equation for the urea-formaldehyde resin plugging system. This discerning analysis illuminates the nuanced shifts in the microscopic reaction mechanism of the urea-formaldehyde resin plugging system. Furthermore, the pressure bearing plugging capacity of the resin plugging system for fractures of different sizes is also studied. It is found that the resin plugging system can effectively resident in parallel and wedge-shaped fractures of different sizes, and form high-strength consolidation under certain temperature conditions. The maximum plugging pressure of resin plugging system for parallel fractures with outlet size 3 mm can reach 9.92 MPa, and the maximum plugging pressure for wedge-shaped fractures with outlet size 5 mm can reach 9.90 MPa. Consequently, the exploration and application of urea-formaldehyde resin plugging material precipitate a paradigm shift, proffering novel concepts and methodologies in resolving the practical quandaries afflicting drilling fluid plugging.

1. Introduction

With the exploration and development of oil and gas fields expanding to a deeper level, lost circulation will become more sudden and complex. Deep and ultra-deep fractures are commonly developed, loss occurs frequently during drilling, and the success

* Corresponding author.
E-mail address: smart-byron@163.com (Y.-R. Bai).

https://doi.org/10.1016/j.petsci.2024.04.016

rate of lost circulation control is low (Sun et al., 2021). The existing domestic technology and the comprehensive introduction of foreign technology have not been solved, which has become the first major technical problem restricting the quality and efficiency of oil and gas drilling engineering (Xu et al., 2023). Losses during drilling can cause the rig to be unable to drill properly, greatly increase the non-productive time, and cause significant economic losses. According to statistics, companies such as CNPC, Sinopec, CNOOC, and Yanchang Petroleum have suffered direct economic losses of over 10 billion yuan annually due to lost circulation (Sun et al., 2021). In recent years, the lost circulation has resulted in an average annual loss time exceeding 4000 days, constituting over two-thirds of the cumulative complex loss time due to drilling accidents. Moreover, the average annual direct economic loss stemming from this issue surpasses 5 billion yuan (Pu et al., 2022). Despite the remarkable progress made in plugging technology in recent years, there is still a notable deficiency in effectively addressing challenging lost circulation reservoirs, especially when confronted with extensive cavernous areas and exceptional fractures (Lei M. et al., 2022; Sun et al., 2021). Consequently, it is of utmost importance to urgently and thoroughly investigate the mechanisms behind drilling fluid loss and plugging, as well as to examine the durability of plugging materials under extreme conditions of high temperatures and pressures, while also assessing their retention and filling capabilities (Kang et al., 2023).

Among the commonplace plugging materials, bridging agents, high water loss compounds, and gels occupy a crucial position, adeptly mitigating the risks associated with drilling fluid loss and significantly enhancing the success rates of plugging operations (Bai et al., 2023a, 2023b; Lashkari et al., 2023; Yang et al., 2023). Bridging plugging materials are composite plugging materials formed by inert materials such as granular, fibrous and sheet according to certain mass ratio and particle size gradation (Xu et al., 2022). Commonly used bridging materials are walnut shell, calcium carbonate, fiber, mica sheet and so on. However, there exists a poor correlation between the particle size of typical bridging plugging materials and the dimensions of the formation's loss channels. This mismatch poses a challenge, as these materials struggle to remain in place within large fractures characterized by extensive crack widths and significant longitudinal extensions, particularly in karst caves (Lashkari et al., 2023). Consequently, this results in a reduced pressure-bearing capacity of the plugging layer. High water-loss plugging materials are generally composed of polymer, diatomaceous earth, cement, sepiolite, attapulgite, asbestos powder, stone ridge, percolating materials and inert materials in a certain proportion (Nguyen et al., 2023). High water-loss plugging materials are easy to use, quick to effect, and have a high success rate in high permeability formation (Sun et al., 2021). However, the high water-loss type plugging materials are similar to bridge type plugging materials, which have poor adaptability to lose channels and are difficult to stay in large fractures or karst caves (Zhou et al., 2022). Gel plugging materials are primarily employed to create robust gels with a three-dimensional network structure, either through chemical crosslinking reactions or by harnessing the intermolecular interactions to effectively plug the loss channels encountered in complex formation drilling fluids (Yang et al., 2023). When compared to other plugging materials, gel plugging materials exhibit superior adaptability to various scales of loss channels, unhindered by shape constraints due to their exceptional deformability under pressure. Moreover, they facilitate the formation of high-strength plugs within these channels, making them a highly effective solution (Bai et al., 2023a). However, these materials are not suitable for reservoirs with large fractures and caves under the condition of deep high temperature and high pressure (Folayan et al., 2023; Lei et al., 2021). The resin plugging material has excellent properties such as heat resistance, pressure resistance and non-flammability, so it can be used as a plugging material alone or coated on the surface of bridging materials such as mica, fiber, walnut shell, quartz sand and so on. Nestled within the embracing warmth of the sidewall temperatures, the consolidation strength undergoes a significant surge, thereby enhancing the likelihood of successful plugging (Chukwuemeka et al., 2023; Garcia et al., 2023).

The thermosetting resin will form a cross-linked network structure during the curing process (Batista et al., 2021). It is characterized by high temperature resistance, high pressure resistance, not easy to burn, stable product size, but its brittleness. Currently, there are mainly several thermosetting resins, such as unsaturated polyester resin, epoxy resin, phenolic resin, urea-formaldehyde resin and so on (Tamez and Taha, 2021; Xiao et al., 2020; Yamanaka et al., 2021). Jiang et al. prepared SA/MPF-E44 composite microcapsules with sodium alginate/melamine phenolic resin as shell and epoxy resin as core by in-situ polymerization (Jiang et al., 2021). The resultant melamine phenolic resin, finely attuned through meticulous modifications, emerged as a paragon of mechanical and thermal stability, embodying the essence of a consummate self-repairing material. Sousa et al. modified unsaturated polyester resin with nano-Al_2O_3 and ZrO_2 particles, and obtained unsaturated polyester resin composites with significantly enhanced mechanical properties (Sousa et al., 2017). The traditional cement slurry plugging material is composed of gypsum, portland, cement, lime and other materials. Due to cement's considerable specific gravity, its hardness upon solidification typically exceeds that of the surrounding stratum. Consequently, during subsequent drilling operations, there is a substantial risk of creating a new wellbore, ultimately leading to the abandonment of the original one (Arbad et al., 2021; Aslani et al., 2022). In addition, the cement slurry will also pollute the drilling fluid, resulting in the failure of the drilling fluid. A layer of resin is coated on the surface of mica, fiber, walnut shell, quartz sand and other materials to aggregate and form phase consolidation after reaching the lost circulation layer. It can effectively enhance the strength of the plugging layer and improve the success rate of primary plugging (Lei S. et al., 2022).

Thermosetting resin material can adapt to different formation temperature and pressure because of its own kind of richness and excellent mechanical properties, heat resistance and chemical resistance after modification (Hofmann et al., 2022; Wang and Ning, 2018; Wang et al., 2022). It has great application potential in the field of oil drilling and production engineering. Li et al. prepared styrene-butadiene resin/nano-SiO_2 composite by continuous emulsion polymerization and used it as a plugging agent for oil-based drilling fluid to improve the plugging efficiency of shale formation (Li et al., 2020). The resin plugging agent can enter the nano-pores of shale formation and significantly reduce fluid invasion, thus improving wellbore stability. Huang et al. synthesized a kind of nano-acrylic resin/nano-SiO_2 composite with core-shell structure for water-based drilling fluid (Huang et al., 2018). It can improve the plugging efficiency of shale pores, reduce fluid invasion and improve wellbore stability in the process of shale gas drilling. Liu et al. prepared nano-SiO_2 modified epoxy resin by in-situ polymerization and added it into cement injection material, which shortened the setting time of composite slurry and improved the stability of composite slurry (Liu W. et al., 2023). Meanwhile, it can delay the hydration of cement and improve the early compressive strength of the composite slurry. Batista and his colleagues employed a polyethylene terephthalate-modified polyester resin as a plugging material, exhibiting remarkable compressive strength and low viscosity (Batista et al., 2021). This innovative material holds promising potential for applications in lost

circulation control, as well as abandonment and remediation operations. Lv et al. prepared an underwater high temperature and slow curing epoxy resin plugging system, which can easily pass through simulated formation fractures and be cured at 120 °C (Lv et al., 2022). The cured epoxy resin has good compressive strength and can effectively plug fractures, which can be applied to drilling fluid plugging during oil and gas drilling. Knudsen et al. prepared a thermosetting resin plugging agent for the successful treatment of heavy oil mud losses in wells of offshore gas fields in the Middle East (Knudsen et al., 2014).

In addition to plugging and modifying the formation, the resin material also has the function of reservoir stimulation, gas well workover, wellbore integrity restoration and old well rehabilitation (Lightford et al., 2006; Purnama, 2011). Sinopec and Shell have successfully applied resin plugging agents to increase reservoir production by 50%, saving up to US$10 million compared to traditional water plugging agents (Li et al., 2020). In the realm of practical engineering, the application of resin plugging agent has a great influence on the effect of sand control (Pal and Banat, 2014). Shell injected resin and proppant into the reservoir to play a role in sand control (de Paiva et al., 2023). Poor cementing quality is easy to cause casing annular air discharge, gas to oil ratio is too high, and oil production is generally low (Safaei et al., 2023). Resin injection is used to block the casing and reduce the proportion of crude oil to more than 1/10, so that the gas well can be put into production again. In the process of oil well maintenance, resin plugging material can be used to repair the oil well to ensure the integrity of the oil well (Liu K. et al., 2023). Marathan Company provides an example of using synthetic resin to repair borehole (Pu et al., 2022). Saudi Aramco has developed a polymer resin system for repair (Gautam et al., 2022), which can improve the mechanical properties of cement paste, especially the shear strength, so as to reduce the annulus pressure of the casing.

Combined with the application characteristics of thermosetting resin with strong deformability before curing and high strength after curing, it can be predicted that thermosetting resin has a broad application prospect in the field of drilling fluid plugging in fractured formation. Therefore, a curing and controllable continuous phase resin plugging material was developed based on the principle of free radical polymerization and chemical synthesis. The resin plugging material is a new type of continuous phase plugging material with easy injection, strong filling, strong retention and high strength underground curing or crosslinking. It is not limited by fracture-cavity lose channels and can meet the basic requirements of different fracture-cavity combination plugging of fracture-cavity carbonate rocks. By comprehensively adjusting the properties of water soluble curable resin and adding filling materials to reduce the cost, a plugging system with high temperature curable resin as the main component was constructed, and its chemical structure was characterized. Meanwhile, combined with the rheological and curing characteristics of the resin plugging system and the pressure plugging effect on fractures of different scales, the curing kinetics and plugging mechanism of the resin plugging system were explored. This study lays a theoretical foundation for the wide application of thermosetting resin plugging materials.

2. Experimental

2.1. Materials

Urea-formaldehyde resin (UF) is a linear urea-formaldehyde oligomer obtained by addition polycondensation of urea and formaldehyde aqueous solution under catalysis. Sodium carboxymethyl cellulose (CMC-Na, 99.9%) and alkyl betaine (BT, 99.8%) are of analytical grade and purchased from Shanghai Mclean Biochemical Company. 3-(methacryloxy) propyltrimethoxysilane (KH570, 97%) is analytical grade and purchased from Aladdin Chemical Reagent Co., Ltd. Ammonium chloride (NH_4Cl, 99.5%), hexamethylenetetramine ($C_6H_{12}N_4$, 98%), sodium chloride (NaCl, 99.5%), calcium chloride ($CaCl_2$, 96%) are all analytical grade and purchased from Sinopharmaceutical Group Chemical Reagent Co., Ltd. Barite (BS, 100~160mesh), purchased from Shandong West Asia Chemical Co., Ltd.

2.2. Preparation of urea-formaldehyde resin

The synthesis process of urea-formaldehyde resin mainly includes two stages: addition reaction and polycondensation reaction (Fig. 1). The first stage is the addition reaction stage. In the neutral or weakly alkaline environment (pH=7–8) formaldehyde reacts with urea, which is dominated by hydroxymethylurea, dihydroxymethylurea and other polycondensation intermediates. The type and quantity of polycondensation intermediates vary with the molar ratio of urea to formaldehyde. According to the steric hindrance principle of chemical functional groups, the more the number of hydroxymethyl groups, the lower the ability of addition and condensation of residual hydrogen atoms on the amino groups of urea. The ratio of the rate of formation of monohydroxy and dihydroxymethyl urea between formaldehyde and urea is 9:3. The second stage is the polycondensation stage, in which the hydroxymethyl on the hydroxymethyl urea molecule forms a linear or reticular polymer in the form of cross-linking under the acidic condition of pH value of 4–6. These linear and branched-chain polymers can form three-dimensional network products when the resin is cured, and finally get polymethylene urea which is insoluble in water and organic matter, and then continue to react to form a network structure of urea-formaldehyde resin.

2.3. Structural characterization

The chemical structure of resin plugging agent was tested by fourier transform infrared spectroscopy (Nicolet iS50 FT-IR) (Yang et al., 2023). Before testing, the cured resin plugging agent sample is cleaned with deionized water to remove the unreacted part, and then the resin plugging agent sample is dried in a vacuum oven and ground into powder. The sample was prepared by potassium bromide tablet pressing method. The infrared spectrum scanning range was 4000~400 cm^{-1}, the scanning temperature was 25 °C, the resolution was 1 cm^{-1}, and the scanning times was 8 times.

The microstructure of the cured sample of resin plugging agent was analyzed by DXR intelligent laser confocal laser Raman spectrometer produced by Seamer Fisher Technology Co., Ltd., and the chemical structure of resin plugging agent was determined by the change of Raman displacement.

Thermogravimetric analyzer (TGA550, USA) was used to detect the thermal stability of chemical bonds in resin plugging agent powder. First, put the resin plugging agent into the oven at 105 °C to remove water. During each measurement, the resin plugging agent samples of 10–15 mg were put into a sealed pan and heated from 25 to 600 °C at the rate of 10 °C/min. The experiment was carried out in nitrogen atmosphere of 50 mL/min.

The ^{13}C CP/MAS NMR of the resin plugging agent was completed on the JEOL-ECA400M superconducting nuclear magnetic resonance instrument. The CP/MAS solid double resonance probe, 3.2 mm ZrO_2 rotor, MAS rotational speed of (15 ± 0.003) kHz and ^{13}C detection resonance frequency of 100.63 MHz were used. The dipole dephasing experiment was carried out after CP. The chemical shift was calibrated with the standard HMB (hexamethylbenzene). The sampling time was π/10 s, the pulse width was 0.478 μs, the

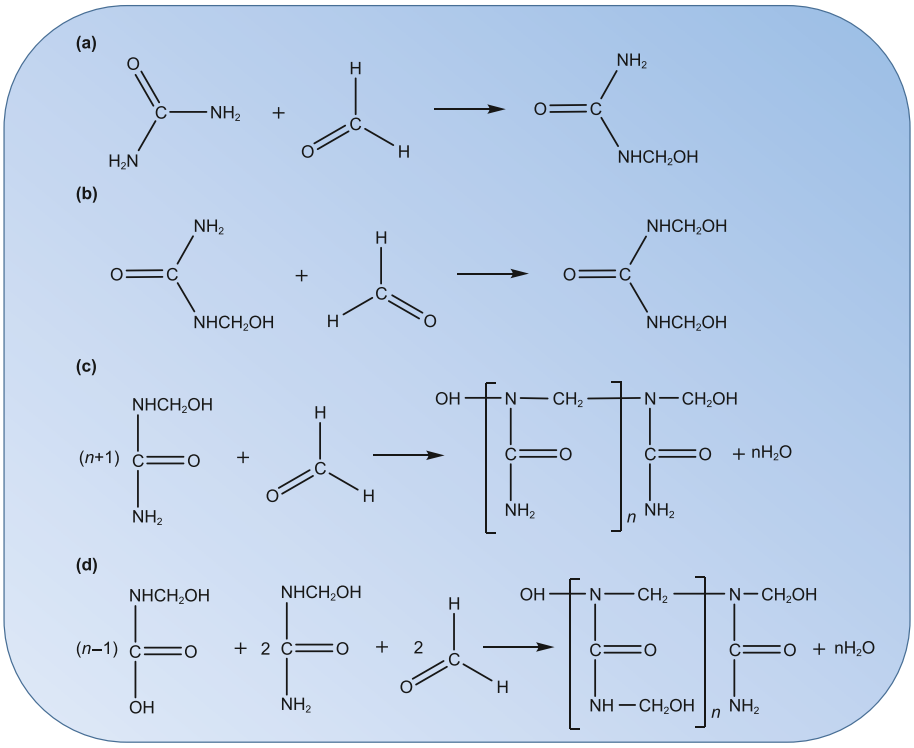

Fig. 1. Equation of addition polycondensation of urea-formaldehyde resin.

cycle delay time was 20 s, and the scanning times was 40000 times.

The microstructure of the resin plugging agent was characterized by Hitachi S-4700 field emission scanning electron microscope (SEM). Carefully cut off the treated resin plugging agent sample to obtain a new cross section. It is then mounted on the aluminum root and sprayed with a thin layer of gold for scanning. Scanning electron microscope imaging was performed under 10 kV.

TEM images were obtained by JEM-2100UHR transmission electron microscope instrument, which works at 120 kV acceleration and is equipped with GATAN-832CCD monitor and EDAX XM2-30 X-ray spectrometer (Yang and Hou, 2020). A sample solution of about 5 μL was injected into the carbon coating porous film by microinjection to obtain the mesh formed across the film. After 10 s, the sample was immediately immersed in ethane at −165 °C. Finally, the sample is transferred to liquid nitrogen (−196 °C) and reversed until it is observed.

2.4. Rheological property

The rheological properties of the samples before curing of resin plugging agent system were tested by HAAKE MARS 60 rotary rheometer. The rotor used in the experiment is CC41/Ti (the diameter of the rotor is 41 mm). The temperature of the test sample is balanced for at least 30 min, and the temperature error is controlled at ±0.1 °C. The apparent viscosity, storage modulus (G') and loss modulus (G'') of resin plugging agent samples in linear viscoelastic region were measured experimentally. The strain range is $\gamma = 0.1\%–1000\%$, and the frequency range is 0–20 Hz. In order to ensure the accuracy of the data, the above rheological properties tests were repeated three times.

2.5. Compressive strength

The urea-formaldehyde resin plugging material was solidified into a cylinder with a bottom diameter of 10 mm and a height of 10 mm. The compression mechanical properties were tested by electronic universal testing machine (CMT4000 electronic universal testing machine, Shenzhen New Sansi material testing Co., Ltd.) at room temperature. The compression speed was set to 3 mm/min, and the stress-strain curve of the resin sample was recorded.

2.6. Differential scanning calorimetry

The curing kinetics of resin plugging agent was studied by differential scanning calorimetry (DSC). The sample of 7–10 mg was accurately weighed and put into the DSC instrument for temperature programmed scanning. The reference crucible was the same type of empty crucible. The detection conditions are as follows: four groups of different heating rates (β): 5, 10, 15, 20 °C/min. Under the condition of N_2 atmosphere, the flow rate is 50 mL/min and the test temperature range is 25–300 °C.

2.7. Plugging performance

The pressure bearing capacity of plugging materials is one of the important parameters to evaluate the plugging effect (Bai et al., 2023a). The plugging performance of curable resin to fractures was studied by using high temperature and high pressure fracture physical simulation device (Fig. 2). The simulated fracture core is made of steel and the appearance is columnar. The fracture runs through the longitudinal section of the steel column. The fracture length is 30 cm, the fracture height is 3 cm, and the fracture width is 3, 5, 7 and 10 mm respectively. The plugging test steps are as follows: (a) Adjust the temperature of the heating box to the simulated formation temperature 130 °C as required. (b) Put the steel fractured core with the required fracture width into the core holder and add confining pressure to 10 MPa. (c) Inject simulated drilling fluid into the fractured core at the injection rate of 10.0 mL/min

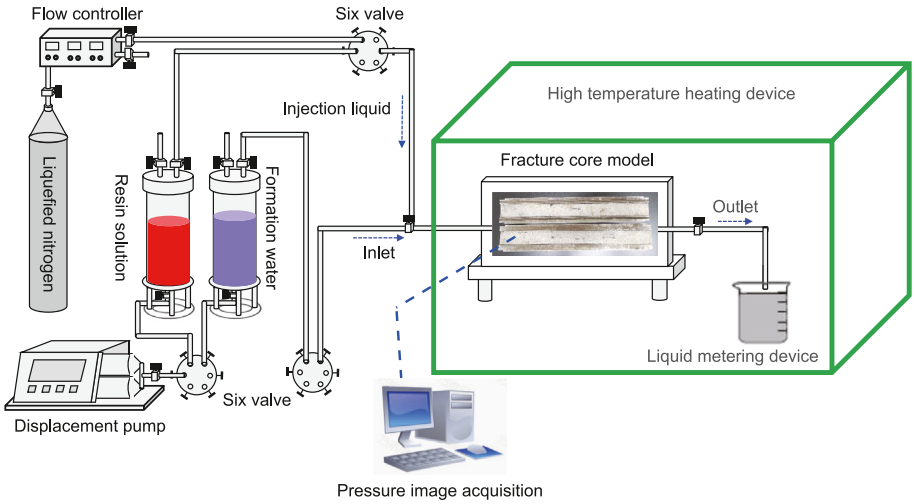

Fig. 2. Plugging device for high temperature and high pressure fractured core.

until it is saturated. (d) The curable resin solution is injected into the fracture core at the injection rate of 10.0 mL/min until the resin solution is completely produced at the fracture outlet and no more aquatic products are produced. (e) The fracture core model is plug and left for 8 h until the resin solution has finished reaction. (f) Reverse injection of simulated drilling fluid into the fracture core at the injection rate of 10.0 mL/min. The change of injection pressure is recorded in real time by using data software, and the highest pressure achieved is the pressure bearing capacity of resin to fractures.

3. Results and discussion

3.1. Synthesis and optimization of resin plugging system

3.1.1. Synthesis of resin plugging system

Employing the methods of physical blending and chemical modification, controllable curing resin plugging materials were meticulously prepared through solution ring-opening polymerization. This involved the strategic utilization of a water-soluble urea-formaldehyde resin as the resin matrix, sodium carboxymethyl cellulose and dodecyl dimethyl betaine as flow pattern regulators, a low molecular weight silicone compound as the resin cross-linking agent, ammonium chloride and hexamethylenetetramine as curing agents, and the judicious incorporation of inorganic suspension materials. The reaction process is shown in Fig. 3. During curing, the active groups such as hydroxymethyl, amide bond and dimethylene ether bond in the resin will cross-link with formaldehyde to form a three-dimensional network structure. Meanwhile, there is free formaldehyde in urea-formaldehyde resin, and the addition of curing agent ammonium chloride reacts with free formaldehyde in urea-formaldehyde resin. Hydrochloric acid was generated through the reaction of ammonium chloride with water and its subsequent thermal decomposition, resulting in a swift reduction of the pH value within the urea-formaldehyde resin. This, in turn, triggered the curing of weak acids, a gradual increase in molecular weight, and the ultimate formation of a network structure resin. The addition of flow pattern regulator can increase the viscosity and shearing force of resin solution and improve the rheological morphology of resin solution. The cross-linking agent of low molecular weight organosilicon compounds contains epoxy, alkoxy and other active functional groups, one end of which can react with the silanol groups on the surface of inorganic materials to form covalent bonds, and the other end can form covalent bonds with resins. Two incompatible materials can be crosslinked to form a network structure.

3.1.2. Formula optimization of resin plugging system

According to the performance requirements of plugging materials in lost circulation control technology, the plugging system of controllable curing resin is determined to be composed of resin matrix, modifier, flow pattern regulator, crosslinking agent, curing agent and suspension agent. In order to further optimize the formula of the resin plugging system, the optimal ratio was obtained by orthogonal test by changing the resin concentration, flow pattern regulator, cross-linking agent, curing agent and so on. The orthogonal test scheme is shown in Table 1.

Through the above orthogonal test single factor analysis, with the gradual increase of urea-formaldehyde resin concentration, the curing time is gradually shortened, as shown in Fig. 4(a). As the resin concentration reaches its zenith at 25%, the pinnacle of plugging prowess is achieved, with a tantalizingly brief curing time of 312 min, ensuring the fulfillment of drilling needs. The addition of modifier can directly introduce hydrophilic groups or chain extenders containing hydrophilic groups into the urea-formaldehyde resin prepolymers for chemical modification. After the urea formaldehyde resin is dissolved in water, the hydrophilic groups in the molecule are oriented towards the water phase and can be stably dispersed in water (Dorieh et al., 2022). As Fig. 4(b) unveils its secrets, when the modifier concentration is 1%, the curing time is 200 min, and the curing effect is better. Increasing the concentration of modifier and shortening the curing time can increase the risk of drilling. Two incompatible materials can be crosslinked to form a network structure by selecting a low molecular weight organosilicon compound cross-linking agent with a special structure. As illustrated in Fig. 4(c), the increase of cross-linking agent greatly shortens the curing time of the resin. When the amount of cross-linking agent is 1%, the curing time is 300 min, and when the amount of cross-linking agent is 10%, the curing time is only 160 min. Flow pattern regulator can increase the viscosity and shearing force of resin solution and improve the rheological morphology of resin solution (Bai et al., 2023b). For example, Fig. 4(d) shows the curing effect of resin plugging material after adding different concentrations of flow pattern regulator, and the addition of flow pattern regulator accelerates the curing process to a certain extent. When the concentration of flow pattern regulator

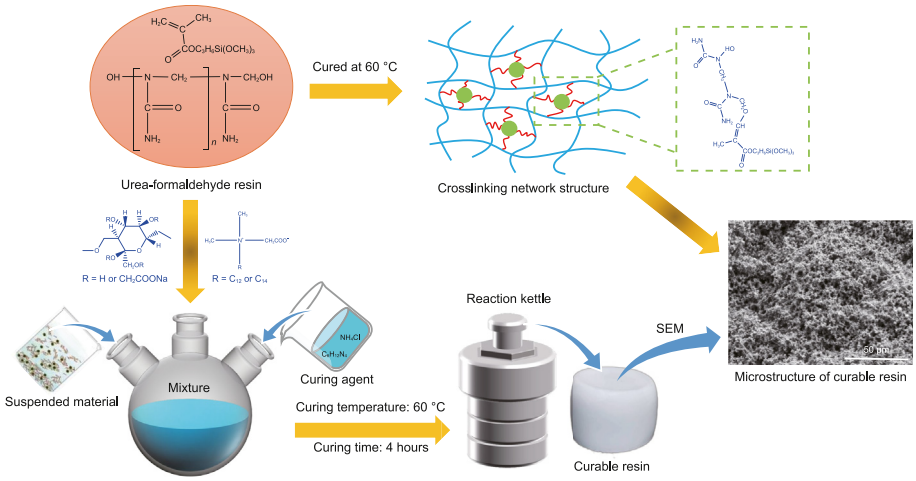

Fig. 3. Schematic diagram of synthesis of curable resin plugging material.

Table 1
Orthogonal test table for optimizing the proportion of resin plugging materials.

Serial number	Resin concentration, %	Modifier, %	Cross-linking agent, %	Flow pattern regulator, %	Curing agent, %	Suspended material, %
1	10	1	1	1	1	1
2	15	2	3	2	2	3
3	20	3	5	3	3	5
4	25	4	7	4	6	7
5	30	5	10	5	10	10

is 1%, the curing time is 189 min, and the curing effect is the best. The addition of curing agent has a significant effect on the curing time of resin materials. As shown in Fig. 4(e), the curing time of resin materials decreases with the increase of curing agent concentration. When the concentration of curing agent is 3%, the curing effect is the best, and the curing time is 180 min. In order to reduce the amount of resin and increase the curing strength of the controllable curing resin, the inorganic suspension material is preferably added to the resin plugging material solution to make it disperse stably. As illustrated in Fig. 4(f), when the amount of suspension material is 5%, the curing time can be controlled at about 383 min, and the curing strength is higher. Through the above orthogonal test results, the optimal formula and proportion of resin plugging system were optimized as follows: 25% urea-formaldehyde resin +1% modifier +1% flow pattern regulator +1% cross-linking agent +3% curing agent +5% suspension material. The curing time is 180~400 min and the curing temperature is 60 °C.

3.2. Structural characterization of resin plugging system

3.2.1. Spectral analysis

In this study, the main functional groups of curable urea-formaldehyde resin prepared with different salinity brine have strong absorption in infrared spectrum. As shown in Fig. 5(a), there is strong absorption of 3000–3500 cm^{-1} (–OH and –NH stretching vibrations), 1630~1700 cm^{-1} (amide I band) and 1500–1600 cm^{-1} (amide II band) in the infrared spectra of urea-formaldehyde resin. Meanwhile, all urea-formaldehyde resins contain hydroxymethyl and ether bonds, which have a wide and strong absorption between 1150 and 1000 cm^{-1} (among them, 1020 cm^{-1} is from $-CH_2OH$, 1070 cm^{-1} near $-CH_2OCH_2-$). In addition, the absorption with variable intensity near 840 cm^{-1} is also characteristic of methylene ether bond, and the medium-strong absorption in the range of 780–800 cm^{-1} is considered to be the skeleton vibration of Uron ring. The formation of intermolecular hydrogen bonds between hydroxyl groups, amino groups, and combinations thereof within pulse aldehyde resin gives rise to the phenomenon of association. Consequently, this association leads to a shift in the stretching vibration absorption peak of H and NH towards the low wavenumber direction, resulting in a prominent and broadened absorption peak centered approximately at 3350 cm^{-1}. 1655 cm^{-1} originates from amide I band and 1540 cm^{-1} is amide II band, which originates from the coupling of bending vibration of NH bond in plane and partial stretching vibration of C–N bond. With the progress of the reaction, the characteristic peak of amide II band gradually shifted to low wavenumber. This is because as the reaction goes on, the degree of the reaction increases and the hydrogen on the amino group is gradually consumed. However, due to the formation of the hydrogen bond, the high shift of the peak wavenumber of the amide II band is reduced, and the non-directional S electrons in the hydrogen orbital are increased (Li and Zhang, 2021). This is conducive to bending vibration, not conducive to telescopic vibration. Due to the reaction of active hydrogen of amide group in urea during the addition stage, several characteristic peaks of amide III band appeared in the addition product, which were 1436, 1388 and 1130 cm^{-1} respectively. The amide III bands of urea-formaldehyde resin prepolymers and cured products appear near 1260 cm^{-1}. It shows that the prepolymer is mainly linear structure $-NHCH_2-$, and the cross-linked structure is formed by the reaction of amino hydrogen in $-NHCH_2-$ during curing, so that the content of linear structure decreases. There is an absorption peak near 1134 cm^{-1}, which results from the asymmetric stretching vibration of methylene in $N-CH_2-N$. This shows that a new methylene bridge structure is formed after hydroxymethyl polycondensation. The vicinity of 1039 and 812 cm^{-1} is attributed to the stretching vibration of

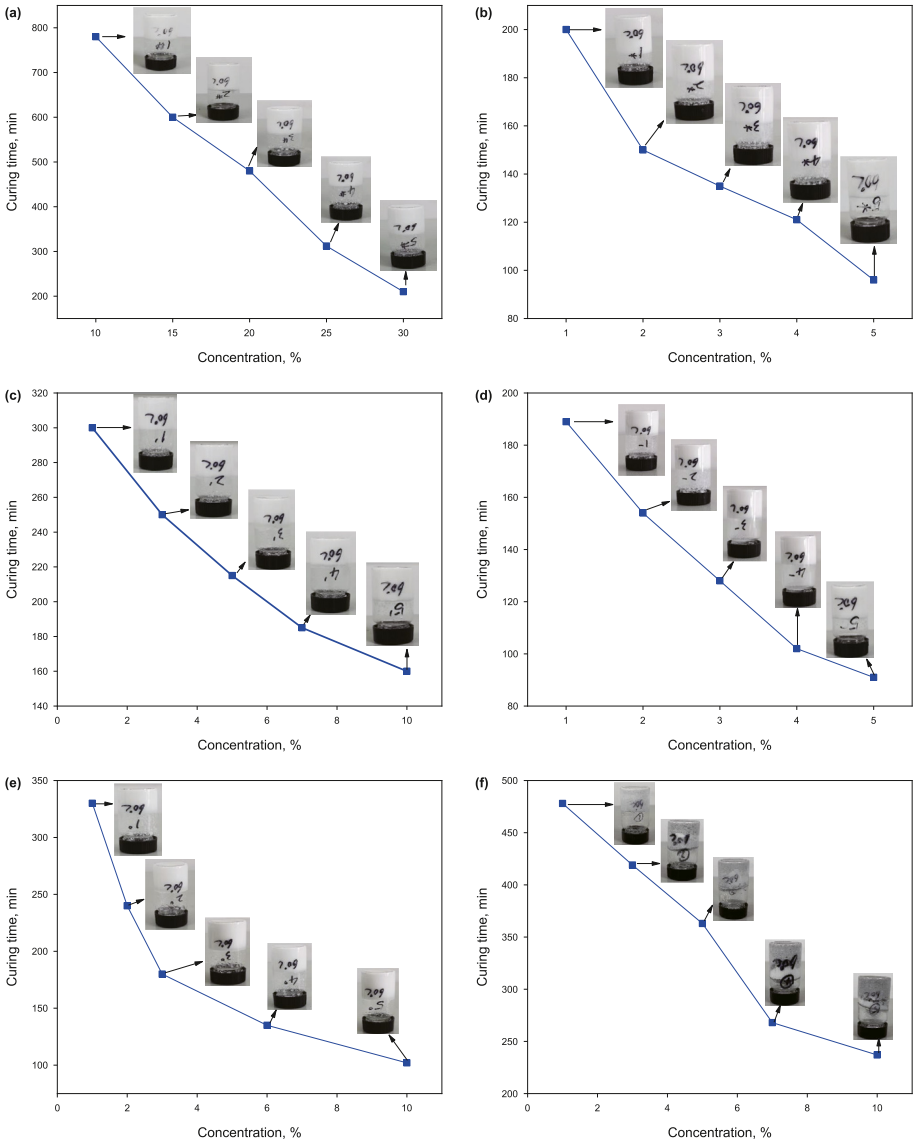

Fig. 4. Optimization of resin plugging materials: (**a**) resin concentration; (**b**) modifier; (**c**) cross-linking agent; (**d**) flow pattern regulator; (**e**) curing agent; (**f**) suspension material.

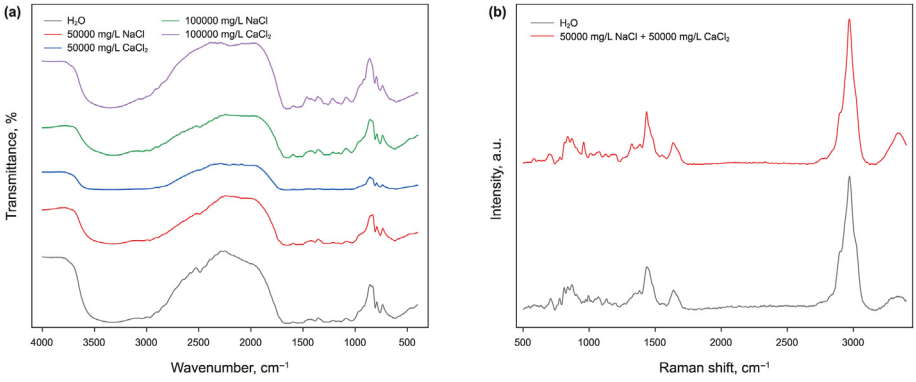

Fig. 5. Spectral analysis of resin plugging materials: (**a**) infrared spectrum; (**b**) Raman spectrum.

C–O bond in ether bond and O–H bond stretching vibration in hydroxymethyl group (–N–CH_2OH–) respectively.

Raman spectra of curable urea-formaldehyde resins is shown in Fig. 5(b). It can be seen from the figure that there are stretching vibration peaks of –OH and –NH at 2967 cm^{-1}. The stretching vibration peak of carbonyl group is mainly shown in

1639–1598 cm^{-1}. 1592–1403 cm^{-1} is the bending vibration peak of CH_2. The bending vibration peak of N–CH_2–N is at 1390 cm^{-1}. 1353–1330 cm^{-1} is the deformation stretching vibration peak of –CH_2, which shows the medium-strong peak of N–CH_2–N. 1205–1041 cm^{-1} is the weak vibration peak of –CH_2OH. 788–998 cm^{-1} is a strong absorption peak of N–CH_2–N. There is an obvious hydroxyl vibration peak at 705 cm^{-1}. The comparative analysis results of infrared spectra and Raman spectra are consistent with the structural characteristics of curable urea-formaldehyde resin samples, indicating that the synthesis achieved the desired purpose.

3.2.2. Thermogravimetric analysis

The thermogravimetric decomposition curves of urea-formaldehyde resin cured samples prepared with brine of different salines are shown in Fig. 6. It can be seen from the figure that the initial pyrolysis temperature and maximum pyrolysis rate of the urea-formaldehyde resin cured prepared with deionized water are 181 and 229 °C at the heating rate of 10 °C/min. The initial pyrolysis temperature and maximum pyrolysis rate of the urea-formaldehyde resin cured with 50000 mg/L NaCl brine were 193 and 241 °C respectively. The initial pyrolysis temperature and maximum pyrolysis rate of the urea-formaldehyde resin cured with 100000 mg/L NaCl brine were 205 and 253 °C respectively. This shows that NaCl salt water can increase the initial pyrolysis temperature of urea-formaldehyde resin cured products. Similarly, we observed that the initial pyrolysis temperature and maximum pyrolysis rate of urea-formaldehyde resin cured by adding 50000 mg/L $CaCl_2$ brine were 199 and 253 °C respectively. The initial pyrolysis temperature and maximum pyrolysis rate of the urea-formaldehyde resin cured with 100000 mg/L $CaCl_2$ brine were 247 and 271 °C respectively. It can be seen that the urea-formaldehyde resin cured with $CaCl_2$ or NaCl brine can increase its thermal decomposition temperature, partially prevent the thermal decomposition of urea-formaldehyde resin, and improve its heat resistance to a certain extent. Meanwhile, $CaCl_2$ has a better effect on increasing the thermal decomposition temperature than NaCl, and the concentration of $CaCl_2$ brine can be appropriately increased when preparing urea-formaldehyde resin curing.

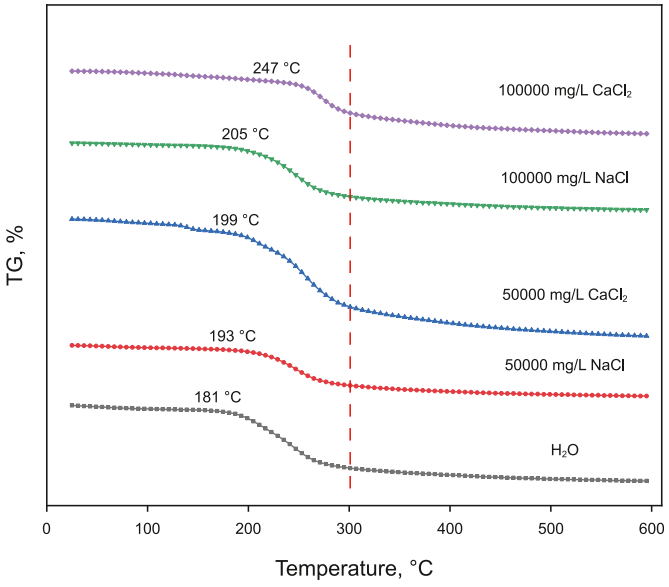

Fig. 6. Thermogravimetric analysis of resin plugging materials.

3.2.3. Solid state nuclear magnetic analysis

^{13}C NMR has been widely accepted as the best method to describe the structure of urea-formaldehyde resin at the molecular level. Since ^{13}C has P electrons outside its nucleus, its extranuclear electrons are mainly paramagnetic shielded. In this case, the range of chemical shifts of various compounds is very wide, and small changes in the structure can cause significant differences in chemical shifts, so the resolution is very high (Liu et al., 2022). Fig. 7 shows the curve of ^{13}C NMR to analyze the structural characteristics of urea-formaldehyde resin cured samples. According to the analysis of ^{13}C NMR spectrum, the signals of various functional groups of urea-formaldehyde resin can be well resolved on ^{13}C NMR. Among them, the absorption of chemical shift 252.3 ppm comes from the carbonyl carbon of urea and its derivatives such as hydroxymethylurea, Uron and so on. The absorption of chemical shift 85.2 ppm originates from methylene ether bonds, including free formaldehyde and its polymers. The absorption of chemical shift −32.7 ppm comes from methylene (–CH_2–). The formation of methylene is beneficial to polycondensation, and the higher the methylene content, the better the hydrolytic stability of the resin. The results of ^{13}C NMR analysis of the structure of urea-formaldehyde resin are basically similar to those of spectral analysis, which shows that the curable urea-formaldehyde resin plugging material is prepared successfully.

3.2.4. Microstructure

The microstructure of urea-formaldehyde resin plugging material was characterized by scanning electron microscope and transmission electron microscope. Based on the synthetic principle of urea-formaldehyde resin plugging material, it can form a high strength consolidation body with reticular structure after cross-linking and curing, which is suitable for high pressure plugging in fractured formation. For this reason, the microstructure of the cured urea-formaldehyde resin plugging material was observed by scanning electron microscope, as shown in Fig. 8(a). It can be clearly seen from the figure that the active groups such as hydroxymethyl, amide bond and dimethylene ether bond in the resin formed a tight spatial network structure after cross-linking with formaldehyde. In order to further observe the microstructure of urea-formaldehyde

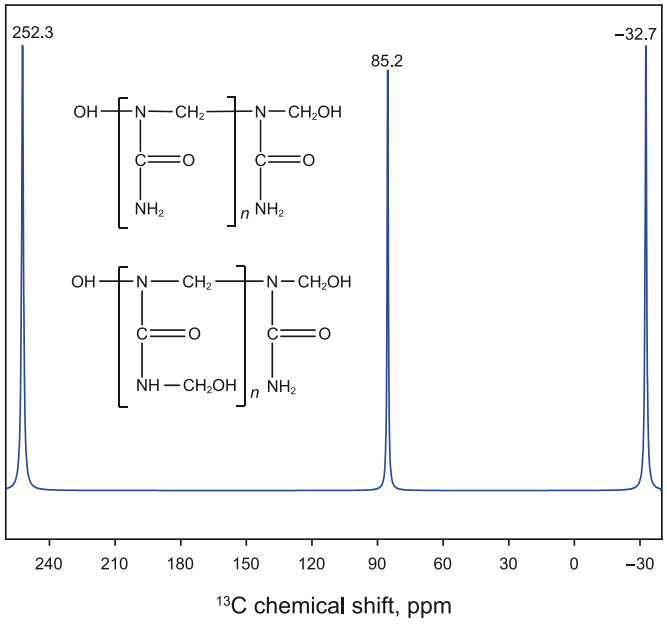

Fig. 7. Solid state NMR analysis of resin plugging materials.

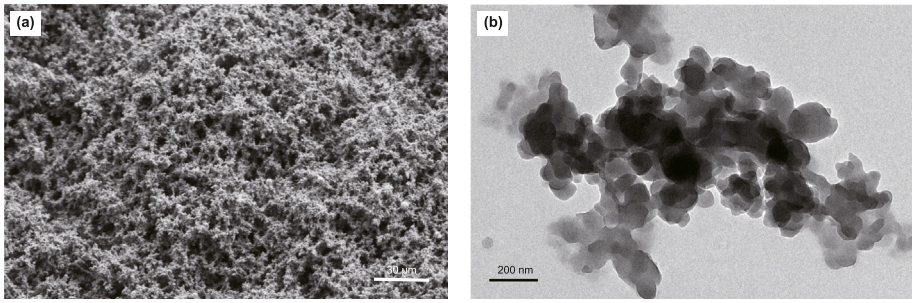

Fig. 8. Microstructure characterization of resin plugging material: (**a**) SEM; (**b**) TEM.

resin plugging material, it was also characterized by high-resolution transmission electron microscope, as shown in Fig. 8(b). It can be seen from the figure that the urea-formaldehyde resin can be closely cross-linked to form a chain-like or reticular structure after curing. The main reason is that the low molecular organosilicon compound with special structure is selected as the cross-linking agent, which contains epoxy group, vinyl group, amide group, alkoxy group and other active functional groups. One end can react with the silanol group on the surface of the inorganic material to form a covalent bond, and the other end can form a covalent bond with the resin, thus crosslinking the two incompatible materials to form a chain-like or reticular structure. In summary, the results of transmission electron microscope and scanning electron microscope are basically the same, which further verifies that the urea-formaldehyde resin plugging material prepared in this study has a tight chain-like or reticular structure.

3.3. Curing performance of resin plugging system

3.3.1. Rheological property of resin plugging system

In this study, HAAKE MARS 60 rheometer was used to test the change of viscosity with shear rate and modulus with shear stress before curing of urea-formaldehyde resin solution with different concentration, as shown in Fig. 9. It can be seen that the solution of urea-formaldehyde resin plugging system shows the characteristics of non-Newtonian fluid. It can be seen from Fig. 9(a) that the viscosity of urea-formaldehyde resin solution prepared by ionized water is less affected by shear rate. The viscosity of urea-formaldehyde resin solution with concentration less than 30% is less than 10 mPa·s, and the viscosity of urea-formaldehyde resin solution with 35% concentration is about 22 mPa·s. It can be seen from Fig. 9(c) and (d) that the addition of NaCl and $CaCl_2$ brine can increase the viscosity of urea-formaldehyde resin solution. The viscosity of 25% urea-formaldehyde resin solution prepared by 500 and 10000 mg/L NaCl salt water is 33 and 26 mPa·respectively, and the viscosity of 25% urea-formaldehyde resin solution prepared by 500 and 10000 mg/L $CaCl_2$ salt water is 91 and 32 mPa·s respectively. Moreover, the urea-formaldehyde resin solution containing NaCl and $CaCl_2$ brine exhibits a pronounced sensitivity to shear rate. As the shear rate escalates, the viscosity gradually decreases. Interestingly, higher salt concentrations result in lower overall solution viscosities. Moving on to Fig. 9(b), which explores the changes in storage modulus and loss modulus of the urea-formaldehyde resin solution under varying shear stress conditions, intriguing observations were made. As the shear stress increases, both the storage modulus and loss modulus of the resin solutions show an upward trend. The loss modulus consistently surpasses the storage modulus, indicating favorable viscous characteristics. These findings validate the favorable flow properties of the urea-formaldehyde resin solution before solidification, making it convenient for pumping during drilling operations while mitigating construction risks. The non-Newtonian behavior of the resin solution adds further complexity to its rheological nature, enhancing its suitability for diverse applications.

3.3.2. Effect of temperature on curing properties

Temperature can affect the curing effect of urea-formaldehyde resin plugging material. It can be seen from Fig. 10(a) that the curing time of urea-formaldehyde resin decreases with the increase of curing temperature. The curing time of urea-formaldehyde resin at 40 °C is 336 min, the curing time at 60 °C is reduced by 35.7%—216 min, and the curing time is only 42 min when the curing temperature continues to rise to 100 °C. However, it should be noted that the cured products formed at higher temperatures, such as 80 and 100 °C, exhibit irregularities and varying degrees of porous structures on their surfaces. This porous morphology compromises the consolidation strength of the urea-formaldehyde resin plugging material to some extent. To further investigate the effect of temperature on the curing process, the compressive strength of the urea-formaldehyde resin cured at different temperatures was evaluated, as depicted in Fig. 10(b). The results reveal a notable trend: the higher the temperature, the lower the compressive strength of the cured urea-formaldehyde resin. The compressive strength of urea-formaldehyde resin cured at 40 °C is 7.3 MPa. The compressive strength of urea-formaldehyde resin cured at 60 °C is 5.8 MPa. The compressive strength of urea-formaldehyde resin formed at 100 °C is only 4.1 MPa. These findings indicate that as the temperature increases, a considerable number of air bubbles form during the resin curing process, resulting in varying degrees of porous structures in the cured products. Therefore, through comprehensive comparative analysis, it is concluded that the best curing temperature of urea-formaldehyde resin plugging material is 60 °C and the curing time is 216 min. At this temperature, the resin exhibits satisfactory compressive strength, fulfilling the plugging requirements in the oil field.

3.3.3. Effect of salt concentration on curing properties

Salt concentration plays a crucial role in the curing performance of urea-formaldehyde resin plugging materials. In this study, different concentrations of NaCl and $CaCl_2$ salt water were utilized to prepare urea-formaldehyde resin plugging materials, and their impact on the curing process was examined. The experimental findings are presented in Fig. 11. Interestingly, it was observed that both NaCl and $CaCl_2$ salt water effectively prolonged the curing time of urea-formaldehyde resin plugging materials. As the concentration of salt water increased, the curing time also lengthened. As depicted in Fig. 11(a), when the concentration of NaCl brine was 500 mg/L, the curing time was 100 min. However, with an increase in NaCl salt water concentration to 100000 mg/L, the curing time

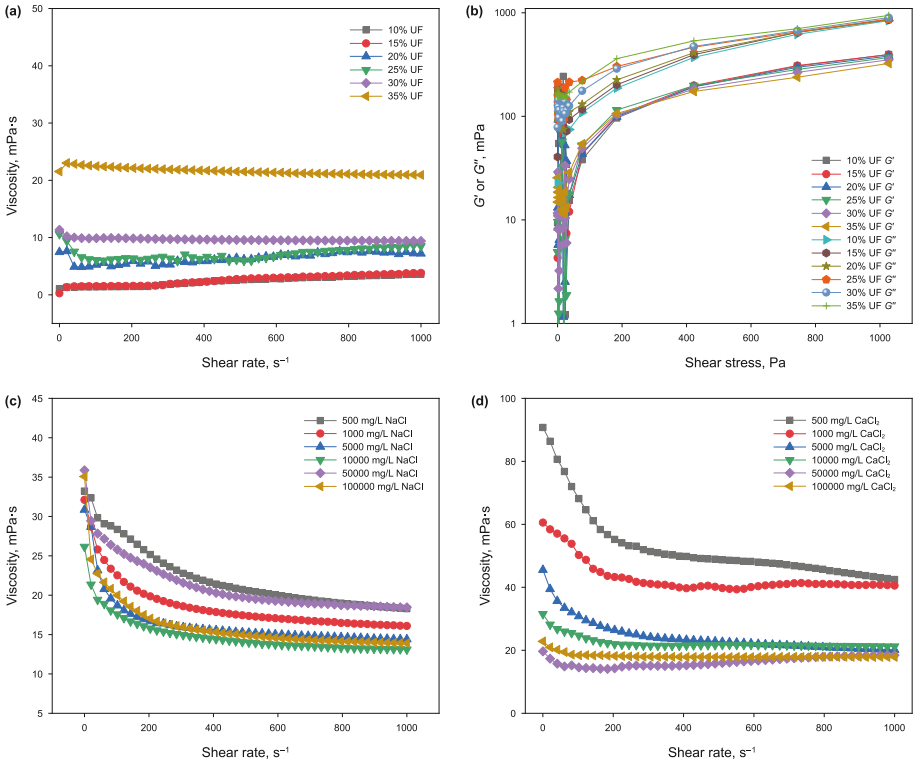

Fig. 9. Rheological properties of resin plugging system: (**a**) the change of viscosity of urea-formaldehyde resin solution of different concentration with shear rate; (**b**) the change of modulus of urea-formaldehyde resin solution of different concentration with shear stress; (**c**) the change of viscosity of urea-formaldehyde resin solution of different concentration of NaCl brine with shear rate; (**d**) the change of viscosity of urea-formaldehyde resin solution of different concentration of $CaCl_2$ brine with shear rate.

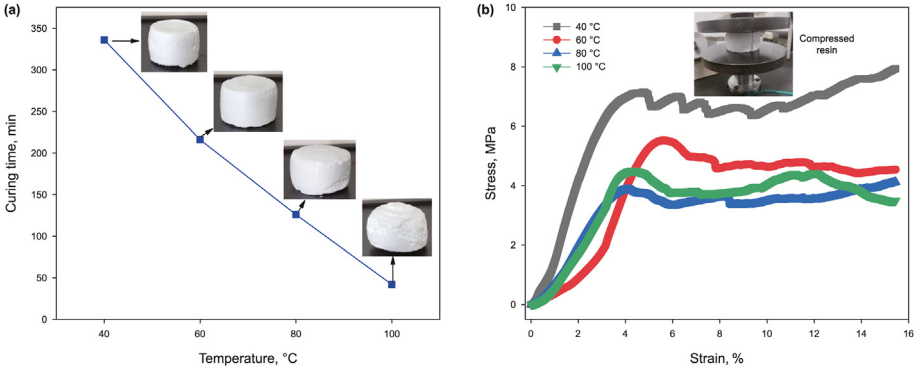

Fig. 10. Effect of temperature on curing effect of resin plugging material: (**a**) effect of temperature on curing time; (**b**) effect of temperature on compressive strength.

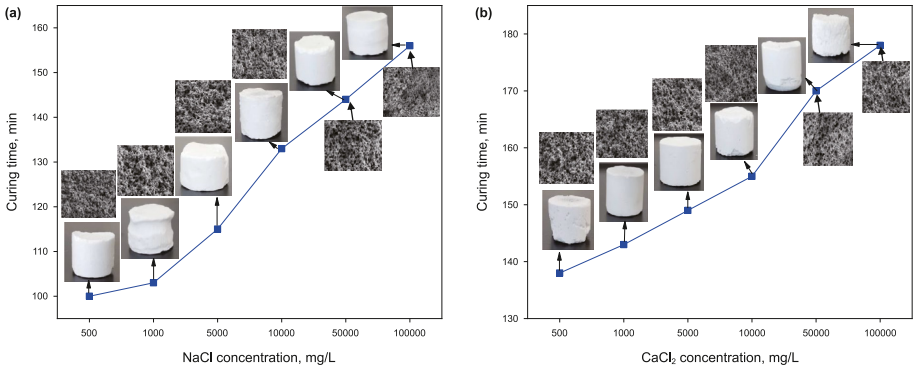

Fig. 11. Effect of salt concentration on curing effect of resin plugging material: (**a**) effect of NaCl brine concentration on curing time; (**b**) effect of $CaCl_2$ brine concentration on curing time.

extended to 156 min, demonstrating a 50% prolongation. Microstructure characterization of the cured urea-formaldehyde resin samples further revealed the presence of a dense network structure, ensuring favorable compressive strength. Fig. 11(b) illustrates the impact of different concentrations of $CaCl_2$ brine on the curing time of urea-formaldehyde resin. The addition of $CaCl_2$ brine also resulted in an extended curing time compared to the control group. Notably, the effect of $CaCl_2$ brine was even more pronounced than that of NaCl brine. At a concentration of 500 mg/L, the curing time reached 138 min. With an increase in $CaCl_2$ salt water concentration to 100000 mg/L, the curing time further increased to 178 min. The microstructure analysis of the solidified urea-formaldehyde resin confirmed the presence of a denser reticular structure, indicative of high-strength plugging capability.

In order to provide further evidence of the impact of salt concentration on the curing effect of urea-formaldehyde resin, a study was conducted to evaluate the effect of NaCl and $CaCl_2$ composite salt water on the curing time of urea-formaldehyde resin at different temperatures. Additionally, the compressive strength of the resulting consolidations was tested, as depicted in Fig. 12. Fig. 12(a) reveals that as the concentration of NaCl and $CaCl_2$ composite salt water increases, the curing time of urea-formaldehyde resin extends. Moreover, a higher proportion of $CaCl_2$ salt water leads to even longer curing times. For instance, the curing time of urea-formaldehyde resin prepared with a compound salt water concentration of 50000 mg/L NaCl +50000 mg/L $CaCl_2$ is 130 min at 40 °C. On the other hand, when the compound salt water concentration is 100000 mg/L NaCl +100000 mg/L $CaCl_2$, the curing time reaches 198 min. These findings highlight the superior effectiveness of compound brine in prolonging the curing time of urea-formaldehyde resin compared to a single saline solution. Furthermore, it is worth noting that the curing time of urea-formaldehyde resin prepared with composite brine decreases with increasing temperature. To further elucidate the effect of composite brine concentration on the curing performance of urea-formaldehyde resin, the compressive strength of the prepared urea-formaldehyde resin consolidations was examined. As illustrated in Fig. 12(b), the compressive strength of the urea-formaldehyde resin prepared with a composite brine solution surpasses that of the single brine solution. Additionally, the compressive strength shows an upward trend with increasing composite brine concentration. For instance, when the concentration of the composite salt water is 50000 mg/L NaCl +100000 mg/L $CaCl_2$, the resin consolidation achieves an impressive compressive strength of 41.5 MPa. In summary, these findings underscore the importance of salt concentration in optimizing the curing performance and mechanical properties of urea-formaldehyde resin plugging materials.

The microstructure of urea-formaldehyde resin consolidations prepared using different concentrations of NaCl and $CaCl_2$ composite salt water is depicted in Fig. 13. A close examination reveals that the urea-formaldehyde resin cured with varying concentrations of NaCl and $CaCl_2$ exhibits a dense network structure, with the density of the cross-linking network increasing as the concentration rises. This can be attributed to the addition of NaCl and $CaCl_2$ composite salt water, which facilitates the cross-linking of low molecular weight organosilicon compounds. Consequently, the active functional groups present in the cross-linking agent undergo full reaction with resins and inorganic materials, resulting in the formation of covalent bonds and an enhancement in the compactness of the reticular structure. Moreover, it is worth noting that the cured structure of urea-formaldehyde resin prepared with compound salt water exhibits a denser configuration compared to that formed using a single salt water solution. Through comprehensive comparative analysis, it is established that when the composite salt water concentration is 50000 mg/L NaCl +100000 mg/L $CaCl_2$, the resulting urea-formaldehyde resin consolidation exhibits a highly compact network structure and boasts exceptional compressive strength. Such characteristics render it suitable for addressing the plugging requirements of drilling fluid losses in fractured formations.

3.4. Curing kinetics of resin plugging system

3.4.1. Theoretical basis

In the practical curing of urea-formaldehyde resin, it is important to consider the varied contributions of different elementary reactions occurring at different stages of the process. The complexity of these reactions makes it challenging to accurately describe the overall curing process. The relationship between activation energy and conversion can be obtained by conversion method. The curing mechanism of urea-formaldehyde resin is revealed from the side (Liu et al., 2021). The degree of curing in urea-formaldehyde resin exhibits a linear correlation with the amount of heat released during the reaction. Eqs. (1) and (2) can be employed to calculate the conversion and reaction rate, enabling a comprehensive understanding of the curing process (Fernández et al., 2009).

$$\alpha = \frac{1}{\triangle H}\int_0^t \frac{\mathrm{d}H}{\mathrm{d}t}\mathrm{d}t \tag{1}$$

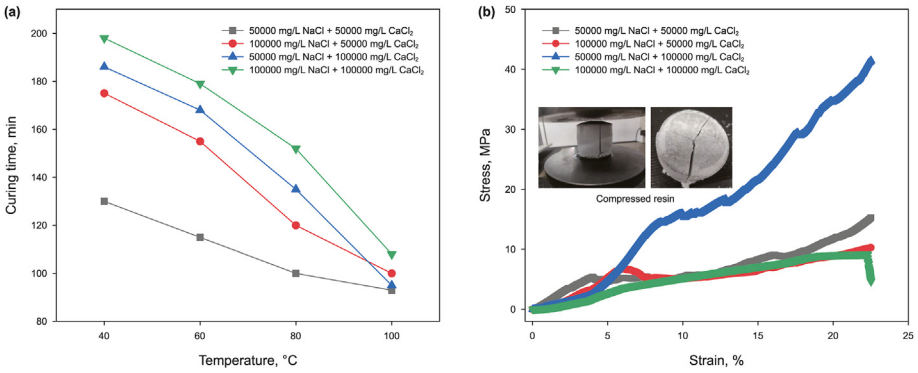

Fig. 12. Effect of composite brine concentration on curing effect of resin plugging material: (**a**) effect of NaCl and $CaCl_2$ composite brine concentration on curing time; (**b**) effect of NaCl and $CaCl_2$ composite brine concentration on compressive strength.

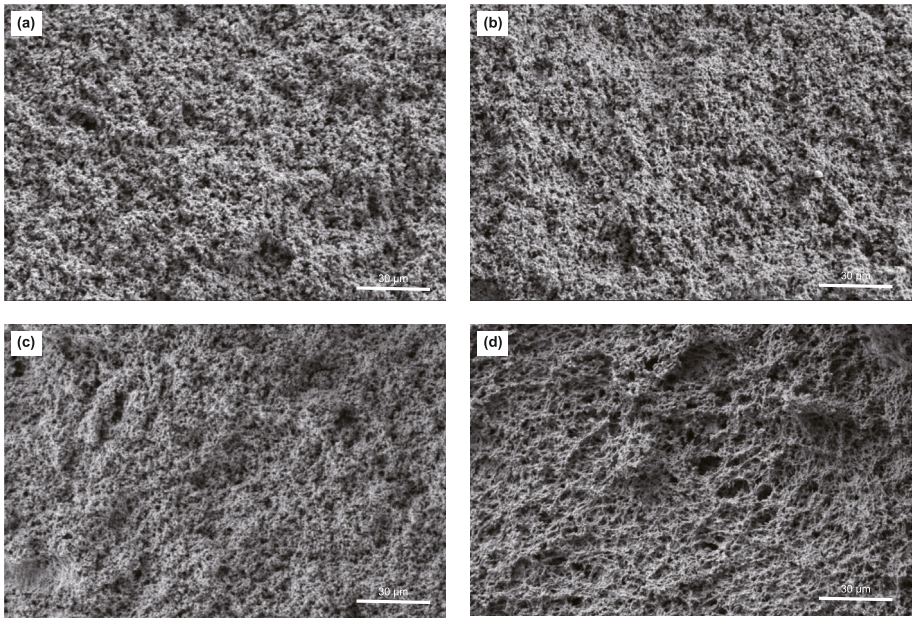

Fig. 13. Microstructure of cured sample of urea-formaldehyde resin plugging material prepared with compound brine concentration: (**a**) 50000 mg/L NaCl+50000 mg/L $CaCl_2$; (**b**) 100000 mg/L NaCl+50000 mg/L $CaCl_2$; (**c**) 50000 mg/L NaCl+100000 mg/L $CaCl_2$; (**d**) 100000 mg/L NaCl+100000 mg/L $CaCl_2$.

$$\frac{d\alpha}{dt}=\frac{dH/dt}{\Delta H}=k(T)f(\alpha) \tag{2}$$

In the formula, α is the conversion rate; dH/dt is the heat flux rate; ΔH is the reaction heat; t is the reaction time; $f(\alpha)$ is the reaction model; $k(T)$ is the reaction rate constant, which obeys the Arehenius law of Eq. (3).

$$k(T)=A\exp\left(\frac{-E_a}{RT}\right) \tag{3}$$

In the formula, A is the pre-exponential factor, E_a is the apparent activation energy, and R is the gas constant, 8.314 J/ (mol·K).

It is worth noting that the complexity of the curing process necessitates the utilization of advanced techniques and mathematical models to capture its intricacies. By investigating the activation energy-conversion relationship and employing conversion methods, researchers can gain a deeper understanding of the underlying curing mechanism in urea-formaldehyde resin. In the realm of resin curing kinetics, Málek et al. have presented a comprehensive approach that offers a systematic solution applicable to the non-isothermal curing reactions of diverse resin systems (Málek, 1992). By examining the relationship between peak exothermic temperature and heating rate at different rates, the data can be analyzed using the Kissinger equation (Eq. (4)) to derive meaningful insights (Málek and Criado, 1994).

$$\ln\left(\frac{\beta}{T_p^2}\right)=\ln\frac{AR}{E_a}-\frac{E_a}{RT_p} \tag{4}$$

In the formula, T_p is the peak exothermic temperature at different rates, and β is the heating rate. Drawing with $\ln(\beta/T_p^2)$ to $1/T_p$, E_a can be calculated according to the linear fitting slope. Then substituted into Eqs. (5) and (6), $y(\alpha)$ and $z(\alpha)$ were constructed to determine the reaction kinetics model.

$$y(\alpha)=\left(\frac{d\alpha}{dt}\right)\exp\left(\frac{E_a}{RT}\right) \tag{5}$$

$$z(\alpha)=\pi(x)\left(\frac{d\alpha}{dt}\right)\frac{T}{\beta} \tag{6}$$

In the formula, $\pi(x)$ is the temperature integral, which is usually calculated by the Eq. (7) derived by Senum and Yang (1977).

$$\pi(x)=\frac{x^3+18x^2+88x+96}{x^4+20x^3+120x^2+240x+120} \tag{7}$$

In the formula, $x=E_a/RT$. The function curves of $y(\alpha)$ and $z(\alpha)$ with respect to α are obtained by substituting the obtained E_a, $d\alpha/dt$, T and β into the Eqs. (5)–(7). According to the normalized $y(\alpha)$ and $z(\alpha)$ function curves, the conversion α_M and α_p^∞ corresponding to the corresponding maximum value and the conversion α_p corresponding to the maximum reaction rate were obtained respectively. Málek's innovative method provides a practical means to characterize and understand the intricacies of resin curing kinetics, particularly in non-isothermal scenarios. By applying this method, researchers can unravel the underlying mechanisms governing resin curing processes, leading to improved understanding and control over curing dynamics in a wide range of applications.

3.4.2. Characteristics of non-isothermal curing reaction

The dynamic behavior of the urea-formaldehyde resin plugging material during the curing process is shown by DSC curve in Fig. 14. Notably, the heating rates employed are 5, 10, 15, and 20 °C/min, respectively. A careful examination of the graph reveals distinct exothermic peaks across all heating curves. This observation implies that, on a macroscopic level, the curing process can be regarded as a kinetic interplay between epoxy groups and amino groups. However, it is essential to acknowledge that the self-polymerization of epoxy groups and the variability in amino activity also exert a certain influence. Through comprehensive analysis of the exothermic curves illustrated in Fig. 14, valuable insights

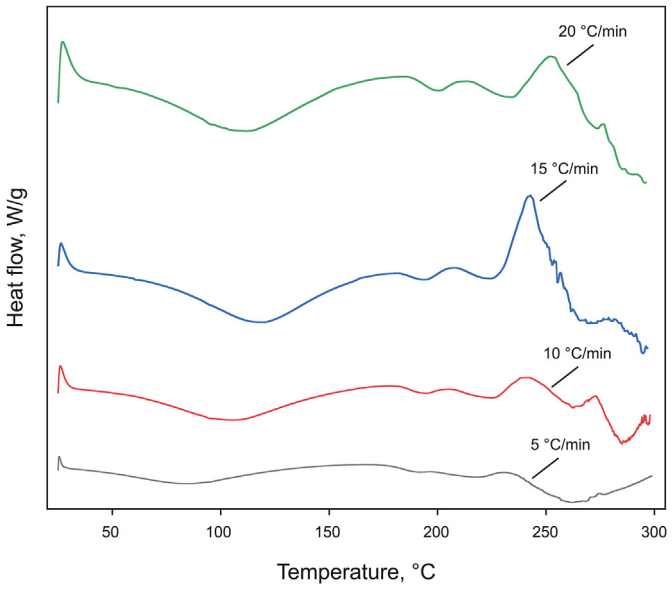

Fig. 14. DSC curves of cured samples of resin plugging materials at different heating rates.

Table 2
Characteristic parameters of curing reaction of resin plugging material.

β, °C/min	ΔH, J/g	T_i, °C	T_p, °C
5	231.5	85.1	177.8
10	240.6	105.7	240.5
15	241.3	116.6	243.8
20	245.5	118.3	252.6

into the heat of reaction during the non-isothermal curing process can be gleaned. Table 2 provides an overview of the characteristic parameters extracted from the non-isothermal curing curves of the resin plugging material at different heating rates. These parameters include the reaction heat (ΔH), initial reaction temperature (T_i), and peak temperature (T_p). Intriguingly, as the heating rate escalates, the exothermic curve widens, accompanied by an increase in both the initial temperature and peak temperature. This phenomenon can be attributed to the heightened heating rate, which exacerbates the temperature lag, thereby resulting in a shift of the curing reaction temperature towards higher values. Furthermore, it is noteworthy that the reaction heat remains relatively stable across different heating rates. This observation suggests that the ultimate reaction degree of the resin plugging material's curing reaction remains largely consistent, irrespective of the employed heating rate. The DSC analysis, accompanied by the corresponding characteristic parameters, provides valuable insights into the non-isothermal curing process of urea-formaldehyde resin plugging material. These findings contribute to a better understanding of the underlying dynamics and behavior of the resin during curing, paving the way for enhanced control and optimization of the curing process in various applications.

3.4.3. Conversion rate

The relationship between the conversion rate of resin plugging materials and temperature is shown in Fig. 15. Notably, the curve exhibits an approximately S-shaped pattern, thus enabling the division of the urea-formaldehyde resin curing process into three distinct stages. In the initial stage, the lower temperature restricts the availability of active sites within the system, consequently leading to a gradual increase in conversion. As the reaction progresses into the middle stage, the ambient temperature rises, triggering autocatalysis phenomena that liberate a substantial amount of heat. This heat release serves as a catalyst for the curing reaction, facilitating a rapid surge in conversion. In the initial stage, the lower temperature restricts the availability of active sites within the system, consequently leading to a gradual increase in conversion. As the reaction progresses into the middle stage, the ambient temperature rises, triggering autocatalysis phenomena that liberate a substantial amount of heat. This heat release serves as a catalyst for the curing reaction, facilitating a rapid surge in conversion. The S-shaped curve depicted in Fig. 15 encapsulates the intricate dynamics of the urea-formaldehyde resin curing process. By comprehending the distinct stages and the underlying factors at play, researchers and practitioners can devise strategies to optimize and control the curing process, ensuring desired outcomes in various resin plugging applications.

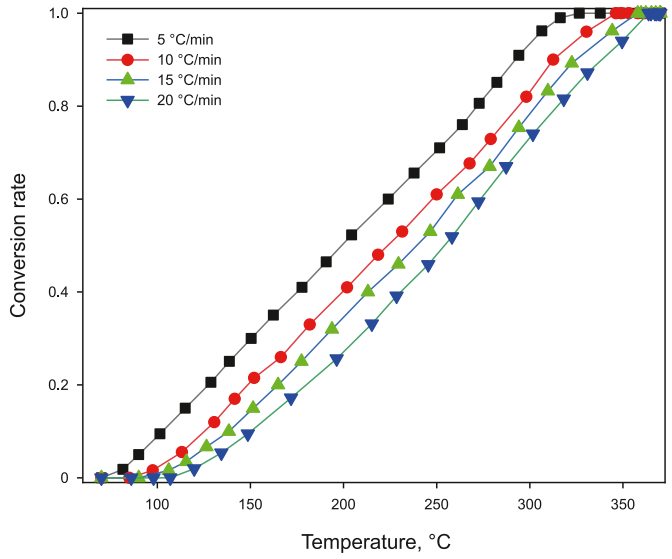

Fig. 15. Relationship between conversion rate of cured sample of resin plugging material and temperature.

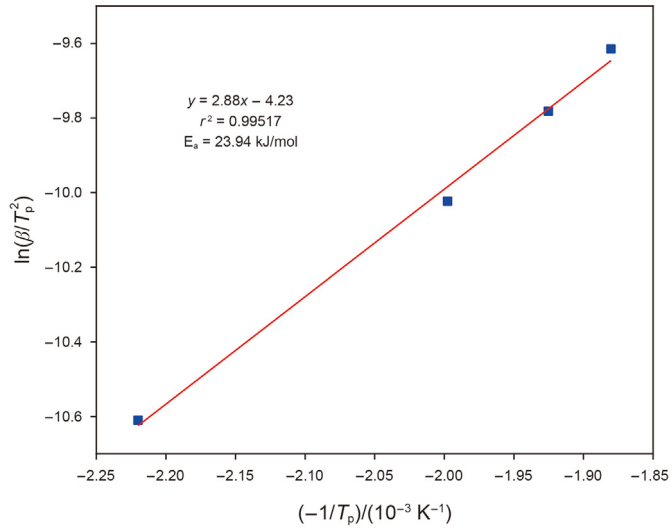

Fig. 16. Relationship between $\ln(\beta/T_p^2)$ and $-1/T_p$ of cured samples of resin plugging material.

3.4.4. Apparent activation energy

The peak temperature T_p and the heating rate β are substituted into the Eq. (4), and the relation curve of $\ln(\beta/T_p^2)$ and $-1/T_p$ is drawn as shown in Fig. 16. By fitting the data points, it can be seen that the linear correlation between the data points is good, and the correlation coefficient is $r^2 = 0.99517$. Therefore, according to Eq. (4), the apparent activation energy of urea-formaldehyde resin plugging material can be calculated to be 23.94 kJ/mol. In comparison to the typical activation energy range of 50–70 kJ/mol observed in epoxy resin systems (Zhang and Vyazovkin, 2005), the apparent activation energy of the urea-formaldehyde resin system is notably lower. This disparity is primarily attributed to the unique molecular structure of the siloxane present in the crosslinking agent of low molecular weight organosilicon compounds. During the curing process, the flexible nature of the siloxane main chain mitigates steric hindrances, facilitating the migration of reaction groups and subsequently leading to a lower apparent activation energy. Conversely, the abundance of rigid segments in epoxy resin systems restricts the movement of chain segments, consequently increasing the apparent activation energy. The identification of this disparity in activation energy between urea-formaldehyde resin and epoxy resin systems sheds light on the underlying molecular dynamics governing the curing processes. This knowledge serves as a valuable guide for researchers and industry professionals seeking to optimize the curing conditions and enhance the performance of resin systems in a variety of applications.

3.4.5. Non-isothermal curing kinetic equation

The relationship between conversion rate and reaction rate of urea-formaldehyde resin curing system at different heating rates is shown in Fig. 17(a). Under different heating rates, the reaction rate of the system increased at first and then decreased, and the maximum reaction rate α_p was between 0.419 and 0.518. With the increase of heating rate, the maximum reaction rate gradually moved to the right. This is attributed to the temperature lag effect. According to Málek method, the above data such as E_a, $d\alpha/dt$, T and β is substituted into Eqs. (5) and (6), and the normalized curves of functions $y(\alpha)$ and $z(\alpha)$ are obtained as shown in Fig. 17(b) and (c), respectively. It can be seen from the diagram that at different heating rates, the normalization curves of $y(\alpha)$ and $z(\alpha)$ basically overlap, and the maximum conversion rates α_M and α_p^∞ are between 0.198–0.215 and 0.467–0.532, respectively.

From the data in Table 3, it can be seen that the conversion characteristic peak value of urea-formaldehyde resin curing system satisfies $\alpha_M < \alpha_p < \alpha_p^\infty$. According to Málek method, it can be determined that the curing kinetics of urea-formaldehyde resin plugging material accords with the $SB(m, n)$ model shown in Eq. (8).

$$\frac{d\alpha}{dt} = A\exp\left(\frac{-E_a}{RT}\right)\alpha^m(1-\alpha)^n \tag{8}$$

In the formula, m and n are the reaction order, and the relationship between them satisfies the Eq. (9).

Table 3
Characteristic peak of conversion of cured samples of resin plugging materials at different heating rates.

β, °C/min	α_p	α_M	α_p^∞
5	0.419	0.198	0.467
10	0.485	0.215	0.493
15	0.493	0.208	0.510
20	0.518	0.201	0.532

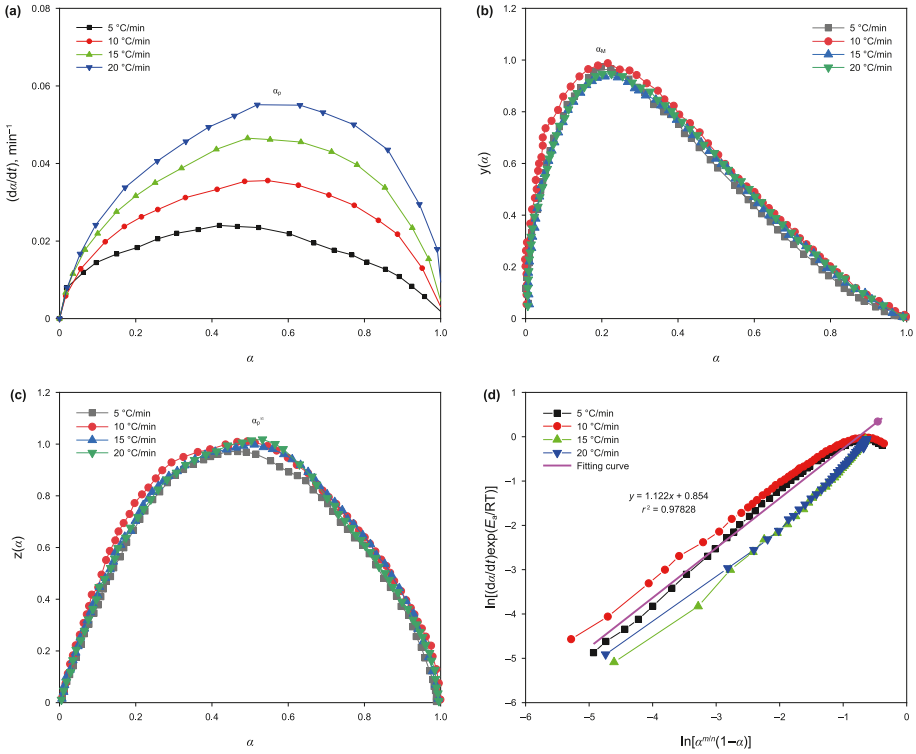

Fig. 17. Functional fitting curves of resin plugging materials at different heating rates: (**a**) conversion α and $d\alpha/dt$; (**b**) $y(\alpha)$ function curve; (**c**) $z(\alpha)$ function curve; (**d**) $\ln[(d\alpha/dt)\exp(E_a/RT)]$ and $\ln[\alpha^{m/n}(1-\alpha)]$ function fitting curve.

$$\frac{m}{n} = \alpha_M / (1 - \alpha_M) \tag{9}$$

The natural logarithms on both sides of Eq. (8) are sorted out:

$$\ln\left[\left(\frac{d\alpha}{dt}\right)\exp\left(\frac{E_a}{RT}\right)\right] = \ln A + n\ln\left[\alpha^{m/n}(1-\alpha)\right] \tag{10}$$

E_a, $d\alpha/dt$, α and m/n are substituted into the Eq. (10), and the relationship between $\ln[(d\alpha/dt)\exp(E_a/RT)]$ and $\ln[\alpha^{m/n}(1-\alpha)]$ is drawn and fitted linearly. The reaction order n, m and $\ln A$ are determined by the slope and intercept of the fitting line, and the complete $SB(m,n)$ model parameters are obtained. Fig. 17(d) shows the linear fitting line of $\ln[(d\alpha/dt)\exp(E_a/RT)]$ for $\ln[\alpha^{m/n}(1-\alpha)]$ when the conversion rate of urea-formaldehyde resin curing system is in the range of 0.1–0.9. It is found that the linearity is good at each heating rate. $A = 2.349$, $m = 0.295$ and $n = 1.122$ are calculated according to the line slope and intercept of the linear fitting curve. According to the calculated results, $m \neq 0$ and n are obviously larger than m, which indicates that both autocatalytic reaction and non-autocatalytic reaction take place in the curing process, and the autocatalytic reaction contributes more to the whole curing reaction. Therefore, the curing kinetic equation of the urea-formaldehyde resin plugging system calculated according to the $SB(m,n)$ model can be obtained by substituting the calculated E_a, $d\alpha/dt$, β, A, m and n into the Eq. (8), as shown in the Eq. (11).

$$\frac{d\alpha}{dt} = 2.349\exp\left(\frac{-23.94}{RT}\right)\alpha^{0.295}(1-\alpha)^{1.122}, \alpha \in [0,1] \tag{11}$$

3.5. Plugging mechanism of resin plugging system

3.5.1. Pressure bearing capacity of resin plugging materials

Once the urea-formaldehyde resin plugging system is injected into the fractured formation, it swiftly finds its place within the fracture space, solidifying and cross-linking under the influence of the formation's temperature. This transformative process culminates in the formation of a robust consolidation body, effectively thwarting any potential drilling fluid loss and ensuring the integrity of the plugging system (Nasr-El-Din and Taylor, 2005). Fig. 18 vividly showcases the exceptional pressure bearing capacity of the urea-formaldehyde resin plugging system when faced with diverse fracture types. It can be seen from Fig. 18(a)–(c) that the urea-formaldehyde resin plugging system can be completely filled in the fractures under the condition of high temperature. Following the completion of the curing process, the resulting consolidation body exhibits remarkable cohesiveness, minimal gravitational settlement, and an evenly distributed structure within the fractures. This consolidation body boasts exceptional toughness and effectively plugs the fractures, providing a reliable barrier against fluid migration. In Fig. 18(d), the plugging pressure of the resin system in parallel fractures and wedge-shaped fractures unfolds before our eyes. With the steady injection of fluid, the plugging pressure gradually mounts until it reaches its zenith, at which point the pressure abruptly drops as the plugging system succumbs to the force exerted by the fluid. Concurrently, the resin plugging material begins to discharge through the core outlet, signifying the deformation and rupture of the urea-formaldehyde resin structure under the strain of fluid pressure. The maximum pressure bearing and plugging capacities of the resin plugging material for different fractured cores are neatly summarized in Table 4. A glimpse at the table reveals that the resin plugging material can withstand an impressive maximum plugging pressure of 9.92 MPa for parallel fractures with an exit size of 3 mm. Likewise, for wedge-shaped fractures with an exit size of 5 mm, the maximum plugging pressure reaches an impressive 9.90 MPa. As the fracture size increases, the plugging pressure diminishes accordingly. Nevertheless, even when confronted with a wedge-shaped fracture boasting a 10 mm exit size, the resin plugging material retains a remarkable maximum plugging pressure of 7.62 MPa, forming a robust plugging layer with exceptional strength. These findings underscore the exceptional performance and versatility of the urea-formaldehyde resin plugging system, cementing its status as a highly effective solution for fracture plugging in a range of applications.

3.5.2. Plugging mechanism of resin plugging materials

In essence, the urea-formaldehyde resin plugging material system exhibits remarkable adaptability to various fracture types, such as parallel and wedge-shaped fractures, as well as different sizes. It adeptly forms high-strength consolidation bodies under specific temperature conditions, delivering an efficient plugging solution (Fig. 19). Comparatively speaking, when considering fractures with identical outlet sizes, the urea-formaldehyde resin plugging system demonstrates a higher breakthrough pressure in wedge-shaped fractures than in parallel fractures. This discrepancy can be attributed to the opposing forces and viscous resistance that the urea-formaldehyde resin plugging system encounters within the wedge-shaped fracture. These counteracting forces effectively impede the erosive impact of the fluid, thereby increasing the maximum breakthrough pressure. In parallel fractures, the

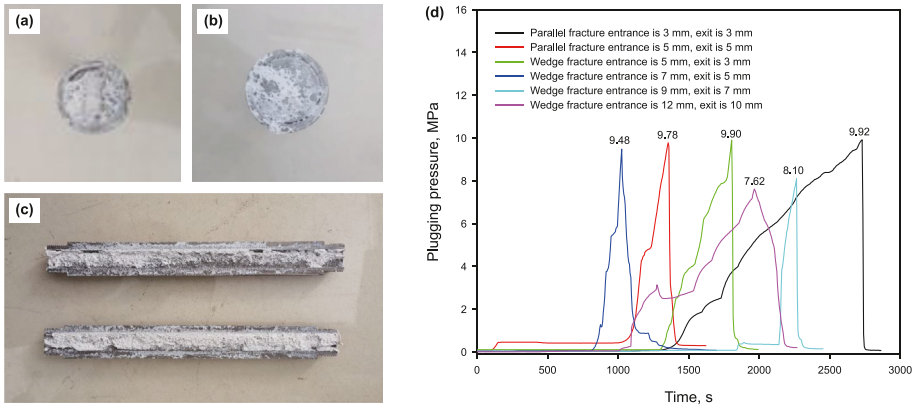

Fig. 18. Plugging experiments with resin plugging materials: (**a**) steel fracture core entrance; (**b**) steel fracture core exit; (**c**) steel fracture core filling profile; (**d**) steel fracture core plugging pressure.

Table 4
Pressure bearing and plugging capacity of resin plugging materials for different types of fractured cores.

Fracture type	Entrance size, mm	Exit size, mm	Plugging pressure, MPa
Parallel fracture	3	3	9.92
	5	5	9.78
Wedge-shaped fracture	5	3	9.90
	7	5	9.48
	9	7	8.10
	12	10	7.62

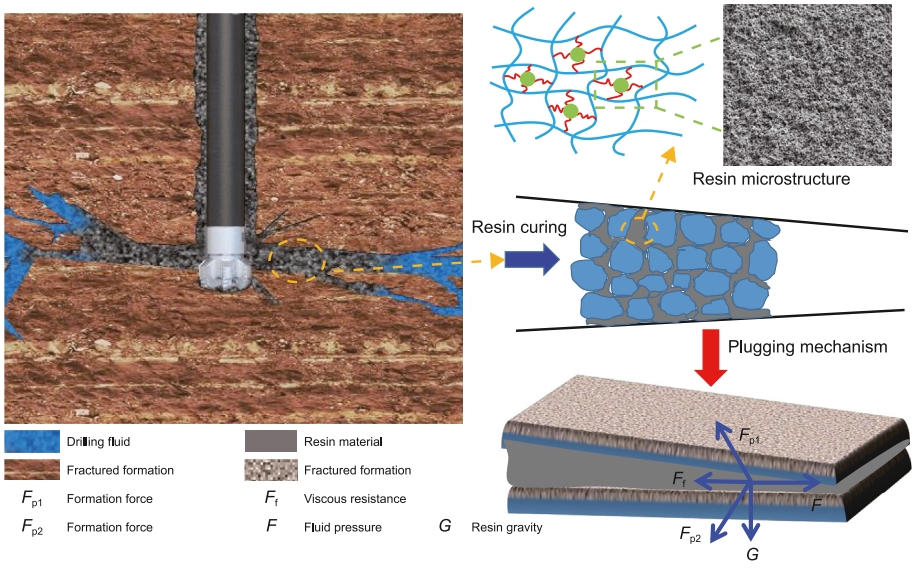

Fig. 19. Schematic diagram of plugging mechanism of urea-formaldehyde resin plugging system in fractured formation.

resistance to fluid impact pressure is primarily attributed to viscous resistance alone, resulting in a relatively lower breakthrough pressure. Additionally, it is worth noting that smaller outlet sizes at the fracture's end yield greater breakthrough pressures for the resin plugging system, subsequently enhancing the overall effectiveness of the plugging process. These observations further underscore the versatility and efficacy of the urea-formaldehyde resin plugging material system, providing valuable insights into its application in a range of fracture types and sizes.

4. Conclusion

In this study, water-soluble urea formaldehyde resin served as the primary plugging material, while a low molecular weight organosilicon compound functioned as the crosslinking agent. Additionally, ammonium chloride and hexamethylenetetramine were employed as curing agents. Through solution step-opening polymerization, a controlled curing resin plugging material with a dense cross-networking structure was meticulously prepared. Its curing time can be adjusted in the range of 3–7 h, which can be used to plug drilling fluid losses of different fracture scales. The resin plugging system showcased exceptional rheological and curing properties. When the concentration of urea-formaldehyde resin remained below 30%, the viscosity of the resin solution clocked in at less than 10 mPa·s, making it an ideal choice for plugging operations. Additionally, the optimum curing temperature of 60 °C demonstrated remarkable salt tolerance. When a composite salt water solution containing 50000 mg/L NaCl and 100000 mg/L $CaCl_2$ was employed, the resulting urea-formaldehyde resin consolidation boasted an even denser network structure, leading to an impressive compressive strength of 41.5 MPa. By delving into the characteristic parameters of the non-isothermal differential scanning calorimetry (DSC) curing reaction, a profound understanding of the relationship between conversion and apparent activation energy was achieved. It was ascertained that the curing kinetic equation of the urea-formaldehyde resin plugging system adhered to the $SB(m,n)$ model. In addition, the resin plugging system exhibited exceptional pressure bearing and plugging capacities across fractures of various sizes. It effectively took up residence within parallel and wedge-shaped fractures of different dimensions, forging robust consolidation bodies when subjected to specific temperature conditions. The maximum plugging pressure for parallel fractures, featuring an outlet size of 3 mm, soared to an impressive 9.92 MPa. Likewise, for wedge-shaped fractures with an outlet size of 5 mm, the maximum plugging pressure reached an equally remarkable 9.90 MPa. The resin plugging material investigated in this study is a continuous phase material that offers effortless injection, robust filling capabilities, exceptional retention, and underground curing or crosslinking with high strength. Its versatility is not constrained by fracture-cavity lose channels, making it suitable for fulfilling the essential needs of various fracture-cavity combinations when plugging fracture-cavity carbonate rocks.

Declaration of competing interest

We declare that we have no financial and personal relationships with other people or organizations that can inappropriately influence our work, there is no professional or other personal interest of any nature or kind in any product, service and company that could

be construed as influencing the position presented in, or the review of, the manuscript entitled.

CRediT authorship contribution statement

Jing-Bin Yang: Writing – review & editing, Writing – original draft, Formal analysis, Data curation. **Ying-Rui Bai:** Writing – review & editing, Writing – original draft, Resources, Methodology, Funding acquisition, Formal analysis, Data curation, Conceptualization. **Jin-Sheng Sun:** Resources, Methodology, Investigation, Funding acquisition, Formal analysis, Data curation. **Kai-He Lv:** Resources, Methodology, Funding acquisition, Formal analysis.

Acknowledgement

This research is financially supported by the National Natural Science Foundation of China (Grant 52374023, 52288101) and Taishan Scholar Young Expert (Grant tsqn202306117).

References

Arbad, N., Rincon, F., Teodoriu, C., et al., 2021. Experimental investigation of deterioration in mechanical properties of oil-based mud (OBM) contaminated API cement slurries & correlations for ultrasonic cement analysis. J. Petrol. Sci. Eng. 205, 108909. https://doi.org/10.1016/j.petrol.2021.108909.

Aslani, F., Zhang, Y., Manning, D., et al., 2022. Additive and alternative materials to cement for well plugging and abandonment: a state-of-the-art review. J. Petrol. Sci. Eng. 215, 110728. https://doi.org/10.1016/j.petrol.2022.110728.

Bai, Y., Yang, J., Sun, J., et al., 2023a. Self-filling and plugging performance of a thixotropic polymer gel for lost circulation control in fractured formation. Geoenergy Science and Engineering 225, 211717. https://doi.org/10.1016/j.geoen.2023.211717.

Bai, Y., Zhu, Y., Sun, J., et al., 2023b. High stability polymer gel for lost circulation control when drilling in fractured oil and gas formations. Geoenergy Science and Engineering 225, 211722. https://doi.org/10.1016/j.geoen.2023.211722.

Batista, W.G.S., Costa, B.L.S., Aum, P.T.P., et al., 2021. Evaluation of reused polyester resin from PET bottles for application as a potential barrier material. J. Petrol. Sci. Eng. 205, 108776. https://doi.org/10.1016/j.petrol.2021.108776.

Chukwuemeka, A.O., Oluyemi, G., Mohammed, A.I., et al., 2023. Plug and abandonment of oil and gas wells – a comprehensive review of regulations, practices, and related impact of materials selection. Geoenergy Science and Engineering 226, 211718. https://doi.org/10.1016/j.geoen.2023.211718.

de Paiva, F.F.G., dos Santos, L.F., Tamashiro, J.R., et al., 2023. Effect of phenolic resin content in waste foundry sand on mechanical properties of cement mortars and leaching of phenols behaviour. Sustainable Chemistry and Pharmacy 31, 100955. https://doi.org/10.1016/j.scp.2022.100955.

Dorieh, A., Selakjani, P.P., Shahavi, M.H., et al., 2022. Recent developments in the performance of micro/nanoparticle-modified urea-formaldehyde resins used as wood-based composite binders: a review. Int. J. Adhesion Adhes. 114, 103106. https://doi.org/10.1016/j.ijadhadh.2022.103106.

Fernández, R., d'Arlas, B.F., Oyanguren, P.A., et al., 2009. Kinetic studies of the polymerization of an epoxy resin modified with rhodamine B. Thermochim. Acta 493 (1), 6–13. https://doi.org/10.1016/j.tca.2009.03.015.

Folayan, A.J., Dosunmu, A., Oriji, B., 2023. Aerobic and anaerobic biodegradation of synthetic drilling fluids in marine deep-water offshore environments: process variables and empirical investigations. Energy Rep. 9, 2153–2168. https://doi.org/10.1016/j.egyr.2023.01.034.

Garcia, C.A., Rosenbaum, E., Spaulding, R., et al., 2023. Numerical approach to simulate placement of wellbore plugging materials using the Lattice Boltzmann method. Geoenergy Science and Engineering 212047. https://doi.org/10.1016/j.geoen.2023.212047.

Gautam, S., Guria, C., Rajak, V.K., 2022. A state of the art review on the performance of high-pressure and high-temperature drilling fluids: towards understanding the structure-property relationship of drilling fluid additives. J. Petrol. Sci. Eng. 213, 110318. https://doi.org/10.1016/j.petrol.2022.110318.

Hofmann, M.A., Shahid, A.T., Garridom, M., et al., 2022. Biobased thermosetting polyester resin for high-performance applications. ACS Sustain. Chem. Eng. 10 (11), 3442–3454. https://doi.org/10.1021/acssuschemeng.1c06969.

Huang, X., Sun, J., Lv, K., et al., 2018. Application of core-shell structural acrylic resin/nano-SiO_2 composite in water based drilling fluid to plug shale pores. J. Nat. Gas Sci. Eng. 55, 418–425. https://doi.org/10.1016/j.jngse.2018.05.023.

Jiang, W., Zhou, G., Wang, C., et al., 2021. Synthesis and self-healing properties of composite microcapsule based on sodium alginate/melamine-phenol–formaldehyde resin. Construct. Build. Mater. 271, 121541. https://doi.org/10.1016/j.conbuildmat.2020.121541.

Kang, Y., Ma, C., Xu, C., et al., 2023. Prediction of drilling fluid lost-circulation zone based on deep learning. Energy 276, 127495. https://doi.org/10.1016/j.energy.2023.127495.

Knudsen, K., Leon, G.A., Sanabria, A.E., et al., 2014. First Application of Thermal Activated Resin as Unconventional LCM in the Middle East. In: International Petroleum Technology Conference. https://doi.org/10.2523/IPTC-18151-MS. IPTC-18151-MS.

Lashkari, R., Tabatabaei-Nezhad, S.A., Husein, M.M., 2023. Evaluation of shape memory polyurethane as a drilling fluid lost circulation and fracture plugging material. Geoenergy Science and Engineering 222, 211445. https://doi.org/10.1016/j.geoen.2023.211445.

Lei, M., Huang, W., Sun, J., et al., 2022. The utilization of self-crosslinkable nanoparticles as high-temperature plugging agent in water-based drilling fluid. SPE J. 27, 1–14. https://doi.org/10.2118/209805-PA.

Lei, M., Huang, W., Sun, J., et al., 2021. Synthesis and characterization of high-temperature self-crosslinking polymer latexes and their application in water-based drilling fluid. Powder Technol. 389, 392–405. https://doi.org/10.1016/j.powtec.2021.05.045.

Lei, S., Sun, J., Bai, Y., et al., 2022. Plugging performance and mechanism of temperature-responsive adhesive lost circulation material. J. Petrol. Sci. Eng. 217, 110771. https://doi.org/10.1016/j.petrol.2022.110771.

Li, J., Zhang, Y., 2021. Morphology and crystallinity of urea-formaldehyde resin adhesives with different molar ratios. Polymers 13 (5), 673. https://doi.org/10.3390/polym13050673.

Li, W., Jiang, G., Ni, X., et al., 2020. Styrene butadiene resin/nano-SiO_2 composite as a water-and-oil-dispersible plugging agent for oil-based drilling fluid. Colloids Surf. A Physicochem. Eng. Asp. 606, 125245. https://doi.org/10.1016/j.colsurfa.2020.125245.

Lightford, S.C., Pitoni, E., Emiliani, C.N., et al., 2006. Rigless interventions in failed gravel-pack gas wells using new resin systems. SPE Prod. Oper. 22 (1), 69–77. https://doi.org/10.2118/98263-PA.

Liu, J., Wang, S., Peng, Y., et al., 2021. Advances in sustainable thermosetting resins: from renewable feedstock to high performance and recyclability. Prog. Polym. Sci. 113, 101353. https://doi.org/10.1016/j.progpolymsci.2020.101353.

Liu, K., Zhu, W., Pan, B., 2023. Laboratory evaluation on oil-soluble resin as selective water shut-off agent in water control fracturing for low-permeability hydrocarbon reservoirs with bottom aquifer. Geoenergy Science and Engineering 225, 211672. https://doi.org/10.1016/j.geoen.2023.211672.

Liu, W., Sun, Y., Meng, X., et al., 2023. Experimental analysis of Nano-SiO_2 modified waterborne epoxy resin on the properties and microstructure of cement-based grouting materials. Energy 268, 126669. https://doi.org/10.1016/j.energy.2023.126669.

Liu, Y., Wang, Q., Xie, Z., et al., 2022. Lycopodiastrum casuarinoides: an overview of their phytochemicals, biological activities, structure-activity relationship, biosynthetic pathway and 13C NMR data. Fitoterapia 165, 105425. https://doi.org/10.1016/j.fitote.2022.105425.

Lv, K., Zhu, Q., Yin, H., et al., 2022. Slow curing of epoxy resin underwater at high temperatures. Ind. Eng. Chem. Res. 61 (46), 16935–16945. https://doi.org/10.1021/acs.iecr.2c02610.

Málek, J., 1992. The kinetic analysis of non-isothermal data. Thermochim. Acta 200, 257–269. https://doi.org/10.1016/0040-6031(92)85118-F.

Málek, J., Criado, J.M., 1994. A simple method of kinetic model discrimination. Part 1. Analysis of differential non-isothermal data. Thermochim. Acta 236, 187–197. https://doi.org/10.1016/0040-6031(94)80267-X.

Nasr-El-Din, H.A., Taylor, K.C., 2005. Evaluation of sodium silicate/urea gels used for water shut-off treatments. J. Petrol. Sci. Eng. 48 (3), 141–160. https://doi.org/10.1016/j.petrol.2005.06.010.

Nguyen, T.T., Sulem, J., Muhammed, R.D., et al., 2023. Experimental investigation of plugging and fracturing mechanisms in unconsolidated sand reservoirs under injection of water containing suspended fine particles. Geoenergy Science and Engineering 221, 211346. https://doi.org/10.1016/j.geoen.2022.211346.

Pal, P., Banat, F., 2014. Comparison of heavy metal ions removal from industrial lean amine solvent using ion exchange resins and sand coated with chitosan. J. Nat. Gas Sci. Eng. 18, 227–236. https://doi.org/10.1016/j.jngse.2014.02.015.

Pu, L., Xu, P., Xu, M., et al., 2022. Lost circulation materials for deep and ultra-deep wells: a review. J. Petrol. Sci. Eng. 214, 110404. https://doi.org/10.1016/j.petrol.2022.110404.

Purnama, G., 2011. Laboratory Studies: Analysis of Resin Composition to Handle Sand Problems on Unconsolidated Gas Formation. In: Proceedings of SPE Annual Technical Conference and Exhibition. Denver, Colorado, USA.

Safaei, A., Asefi, M., Ahmadi, M., et al., 2023. Chemical treatment for sand production control: a review of materials, methods, and field operations. Petrol. Sci. 20 (3), 1640–1658. https://doi.org/10.1016/j.petsci.2023.02.013.

Senum, G.I., Yang, R.T., 1977. Rational approximations of the integral of the Arrhenius function. J. Therm. Anal. 11 (3), 445–447. https://doi.org/10.1007/BF01903696.

Sousa, S.P.B., Ribeiro, M.C.S., Nóvoa, P.R.O., et al., 2017. Mechanical behaviour assessment of unsaturated polyester polymer mortars filled with nano-sized Al_2O_3 and ZrO_2 particles. Ciência & Tecnologia dos Materiais 29 (1), e167–e171. https://doi.org/10.1016/j.ctmat.2016.08.002.

Sun, J., Bai, Y., Cheng, R., et al., 2021. Research progress and prospect of plugging technologies for fractured formation with severe lost circulation. Petrol. Explor. Dev. 48 (3), 732–743. https://doi.org/10.1016/S1876-3804(21)60059-9.

Tamez, M.B.A., Taha, I., 2021. A review of additive manufacturing technologies and markets for thermosetting resins and their potential for carbon fiber integration. Addit. Manuf. 37, 101748. https://doi.org/10.1016/j.addma.2020.101748.

Wang, M., Ning, Y., 2018. Oligosilylarylnitrile: the thermoresistant thermosetting resin with high comprehensive properties. ACS Appl. Mater. Interfaces 10 (14),

11933–11940. https://doi.org/10.1021/acsami.8b00238.
Wang, Y., Hansen, C.J., McAninch, I.M., et al., 2022. Resin wettability correlates linearly to interfacial fracture energy between thermosetting elastomers and glass. ACS Appl. Polym. Mater. 4 (6), 4244–4253. https://doi.org/10.1021/acsapm.2c00217.
Xiao, H., Zhou, T., Shi, M., et al., 2020. A molding-sintering method inspired by powder metallurgy for thermosetting resins with narrow processing window: a case study on bio-based adenine containing phthalonitrile. Chem. Eng. J. 398, 125442. https://doi.org/10.1016/j.cej.2020.125442.
Xu, C., Zhang, H., Kang, Y., et al., 2022. Physical plugging of lost circulation fractures at microscopic level. Fuel 317, 123477. https://doi.org/10.1016/j.fuel.2022.123477.
Xu, C., Zhang, H., She, J., et al., 2023. Experimental study on fracture plugging effect of irregular-shaped lost circulation materials. Energy 276, 127544. https://doi.org/10.1016/j.energy.2023.127544.
Yamanaka, Y., Matsubara, S., Saito, R., et al., 2021. Thermo-mechanical coupled incremental variational formulation for thermosetting resins subjected to curing process. Int. J. Solid Struct. 216, 30–42. https://doi.org/10.1016/j.ijsolstr.2021.01.014.
Yang, J., Sun, J., Bai, Y., et al., 2023. Preparation and characterization of supramolecular gel suitable for fractured formations. Petrol. Sci. 20 (4), 2324–2342. https://doi.org/10.1016/j.petsci.2023.01.011.
Yang, J., Hou, J., 2020. Synthesis of erucic amide propyl betaine compound fracturing fluid system. Colloids Surf. A Physicochem. Eng. Asp. 602, 125098. https://doi.org/10.1016/j.colsurfa.2020.125098.
Zhang, Y., Vyazovkin, S., 2005. Curing of diglycidyl ether of bisphenol P with nitro derivatives of amine compounds, 2. Macromol. Chem. Phys. 206 (11), 1084–1089. https://doi.org/10.1002/macp.200500018.
Zhou, H., Wu, X., Song, Z., et al., 2022. A review on mechanism and adaptive materials of temporary plugging agent for chemical diverting fracturing. J. Petrol. Sci. Eng. 212, 110256. https://doi.org/10.1016/j.petrol.2022.110256.